



OPEN ACCESS

EDITED BY

Ryan C. Fortenberry,
University of Mississippi, United States

REVIEWED BY

Umberto Terranova,
University of Buckingham, United Kingdom
Nathan John DeYonker,
University of Memphis, United States
Marco Fioroni,
University of Memphis, United States

*CORRESPONDENCE

Xiao-Lan Huang,
✉ xiaolan.huang@ymail.com
Gerhard Schenk,
✉ schenk@uq.edu.au

RECEIVED 04 December 2023

ACCEPTED 23 January 2024

PUBLISHED 08 February 2024

CITATION

Huang X-L, Harmer JR, Schenk G and Southam G (2024), Inorganic Fe-O and Fe-S oxidoreductases: paradigms for prebiotic chemistry and the evolution of enzymatic activity in biology.
Front. Chem. 12:1349020.
doi: 10.3389/fchem.2024.1349020

COPYRIGHT

© 2024 Huang, Harmer, Schenk and Southam. This is an open-access article distributed under the terms of the [Creative Commons Attribution License \(CC BY\)](#). The use, distribution or reproduction in other forums is permitted, provided the original author(s) and the copyright owner(s) are credited and that the original publication in this journal is cited, in accordance with accepted academic practice. No use, distribution or reproduction is permitted which does not comply with these terms.

Inorganic Fe-O and Fe-S oxidoreductases: paradigms for prebiotic chemistry and the evolution of enzymatic activity in biology

Xiao-Lan Huang^{1*}, Jeffrey R. Harmer², Gerhard Schenk^{2,3,4*} and Gordon Southam^{4,5}

¹NYS Center for Clean Water Technology, School of Marine and Atmospheric Sciences, Stony Brook, NY, United States, ²Australian Institute of Bioengineering and Nanotechnology, The University of Queensland, Brisbane, QLD, Australia, ³School of Chemistry and Molecular Biosciences, The University of Queensland, Brisbane, QLD, Australia, ⁴Sustainable Minerals Institute, The University of Queensland, Brisbane, QLD, Australia, ⁵School of the Environment, The University of Queensland, Brisbane, QLD, Australia

Oxidoreductases play crucial roles in electron transfer during biological redox reactions. These reactions are not exclusive to protein-based biocatalysts; nano-size (<100 nm), fine-grained inorganic colloids, such as iron oxides and sulfides, also participate. These nanocolloids exhibit intrinsic redox activity and possess direct electron transfer capacities comparable to their biological counterparts. The unique metal ion architecture of these nanocolloids, including electron configurations, coordination environment, electron conductivity, and the ability to promote spontaneous electron hopping, contributes to their transfer capabilities. Nano-size inorganic colloids are believed to be among the earliest 'oxidoreductases' to have 'evolved' on early Earth, playing critical roles in biological systems. Representing a distinct type of biocatalysts alongside metalloproteins, these nanoparticles offer an early alternative to protein-based oxidoreductase activity. While the roles of inorganic nano-sized catalysts in current Earth ecosystems are intuitively significant, they remain poorly understood and underestimated. Their contribution to chemical reactions and biogeochemical cycles likely helped shape and maintain the balance of our planet's ecosystems. However, their potential applications in biomedical, agricultural, and environmental protection sectors have not been fully explored or exploited. This review examines the structure, properties, and mechanisms of such catalysts from a material's evolutionary standpoint, aiming to raise awareness of their potential to provide innovative solutions to some of Earth's sustainability challenges.

KEYWORDS

oxidoreductases, biocatalysts, inorganic nanocatalysts, metal ion architecture, evolution, sustainability, biotechnology

1 Introduction-inorganic abiotic nanocolloids as efficient catalysts of biologically relevant reactions

Oxidoreductases are a superfamily of enzymes (*i.e.*, biocatalysts) found throughout the tree of life (Williams, 1981; Falkowski et al., 2008; Kim et al., 2013). These enzymes are molecular machines responsible for virtually all biologically induced electron transfer (ET) reactions. Examples include peroxidases (PODs), catalases (CATs), superoxide dismutases (SODs) and oxidases (OXDs). Various metabolic pathways, such as glycolysis, the Krebs cycle, photosynthesis in chloroplasts, drug metabolism and detoxification reactions in the liver require oxidoreductases. Reactive oxygen species (ROS) and hydrogen peroxide (H_2O_2) are frequently observed metabolites in reactions catalyzed by oxidoreductases (Apel and Hirt, 2004; Bayr, 2005; Valko et al., 2007; Sharma et al., 2012). PODs use H_2O_2 or organic hydroperoxides (R-OOH) as electron donors and H_2O_2 as electron acceptor during redox reactions (Rodríguez-López et al., 2001; Veitch, 2004; Leblanc et al., 2015; de Oliveira et al., 2021). OXDs catalyze the oxidation of various substrates (electron donors) by using molecular oxygen (O_2) as an electron acceptor. In these reactions, hydrogen atoms are used to form water or H_2O_2 by enzymes such as sulfite oxidase (SOE), glucose oxidase (GOX), or alcohol oxidase (AOX) (Messner and Imlay, 2002; Leskovac et al., 2005; Jancura et al., 2014; Kappler and Enemark, 2015). CATs accelerate the decomposition of H_2O_2 into water and O_2 (Deisseroth and Dounce, 1970; Alfonso-Prieto et al., 2009), while SODs disproportionately divide superoxide radicals (O_2^{*-}) into H_2O_2 and O_2 (Fridovich, 1995; Sheng et al., 2014).

The primary function of biological oxidoreductases is ET, though some oxidoreductases can transfer electrons directly or through mediators such as cytochrome *c* (Cyt *c*), to solid surfaces, including electrodes, enzymes, microorganisms and nanomaterials (Kracke et al., 2015; Milton and Minteer, 2017; Chen H. et al., 2020; Ratautas and Dagys, 2020). This process, known as direct ET (DET) (Kracke et al., 2015; Milton and Minteer, 2017; Chen H. et al., 2020; Ratautas and Dagys, 2020; Suprun, 2021) was first observed in 1977 (Eddowes and Hill, 1977; Peter and Theodore, 1977) for Cyt *c* on gold and tin-doped indium oxide electrodes, exhibiting virtually reversible electrochemistry as revealed by cyclic voltammetry. Horseradish peroxidase (HRP) (Yaropolov et al., 1979) and laccase (Lc) (Tarasevich et al., 1979) have been shown to adsorb on carbon electrodes and exhibit DET capacity. Currently, more than 100 enzymes are known to be capable of working under DET conditions, with the majority being oxidoreductases (Gorton et al., 1999; Ferapontova et al., 2003; Shleev et al., 2005; Liu et al., 2006; Léger and Bertrand, 2008; Liu et al., 2014; Bollella et al., 2018).

Oxidoreductase activity is not limited to protein-based catalysts; some inorganic colloids with oxidoreductase-like activity are able to catalyze biochemical reactions *in vitro* and *in vivo* (Wei and Wang, 2013; Wu J. et al., 2019; Huang et al., 2019; Liang and Yan, 2019; Singh, 2019; Zhang X. et al., 2021; Yang et al., 2021; Hong et al., 2022). It should be noted that inorganic colloids can perform other catalytic functions,

including the hydrolysis of phosphate ester bonds (Huang and Zhang, 2007; Huang and Zhang, 2012; Huang, 2018; Huang, 2019). Some of the best studied inorganic systems are iron oxides such as inorganic peroxidase (*e.g.*, magnetite (Mag, Fe_3O_4) colloids (1-1,000 nm)) that can include a highly reactive nanoparticle (NP) sub-fraction (<100 nm) (Gao et al., 2007; Chaudhari et al., 2012; Chen et al., 2012; Gao et al., 2017; Gao and Yan, 2019; Gao, 2022). Synthetic Mag NPs were the first inorganic nanomaterials reported to possess intrinsic POD-like properties (Gao et al., 2007) catalyzing the oxidation of organic substrates such as 3,3,5,5-tetramethylbenzidine (TMB), diazoaminobenzene (DAB) and o-phenylenediamine (OPD). Displaying Michaelis-Menten-type behavior, their reaction velocity is inversely related to the particle size (*i.e.*, the larger the surface area of the NPs/colloids the greater their activity) (Gao et al., 2007). In terms of their catalytic efficiency (k_{cat}/K_m) some of these abiotic catalysts (H_2O_2 : $560\text{ mM}^{-1}\text{ s}^{-1}$; TMB: $3.1 \times 10^5\text{ mM}^{-1}\text{ s}^{-1}$) are comparable to their biological counterparts (H_2O_2 : $940\text{ mM}^{-1}\text{ s}^{-1}$; TMB: $9.2 \times 10^3\text{ mM}^{-1}\text{ s}^{-1}$) (Gao et al., 2007). Numerous iron oxide colloids have been shown to exhibit similar intrinsic POD activity, including maghemite (Mah, $\gamma\text{-}Fe_2O_3$) (Chen et al., 2012), hematite (Hem, $\alpha\text{-}Fe_2O_3$) (Chaudhari et al., 2012), two-dimensional lepidocrocite nanomaterials formed from graphene-templates (Peng et al., 2011), and Prussian blue-modified iron oxide magnetic compounds (Wang and Huang, 2011). These inorganic catalysts also display substrate selectivity, temperature responsiveness and pH dependence similar to natural enzymes (Gao et al., 2007; André et al., 2011; Huang and Zhang, 2012; Wei and Wang, 2013; Wu et al., 2019; Huang, 2018, 2019, 2022a). This observation has the potential to revolutionize various industries and applications, offering more efficient and customized catalytic processes. The implications for fields such as medicine (Gao and Yan, 2019; Lopez-Cantu et al., 2022; Wei et al., 2023), environmental science (Meng et al., 2020; Wong et al., 2021), and agricultural production (Liu et al., 2021; Cui et al., 2022) are truly exciting.

Inorganic nanocatalysts, possessing enzyme-like activity are not limited to iron oxides and sulfides, *i.e.*, many other metal NPs exhibit properties or functions similar to enzymes. For example, molybdenum disulfide (MoS_2) NPs possess both semiconductor properties (Radisavljevic et al., 2011) and electron hopping behavior (Qiu et al., 2013), allowing them to naturally act as POD, CAT, and SOD (Chen et al., 2018; Yu et al., 2021). Similarly, mixed-valence vanadium pentoxide V_2O_5 NPs exhibit semiconducting characteristics (Sanchez et al., 1983a) due to electron hopping dynamics within V^{4+} and V^{5+} ions (Sanchez et al., 1983b), and also exhibit intrinsic POD, GOX and glutathione peroxidase (GPx) activity (André et al., 2011; Natalio et al., 2012; Ghosh et al., 2018; Ding Y. et al., 2020; Chen, 2022). In MnO_2 NPs, direct electron hops within Mn - Mn chains (Devaraj and Munichandraiah, 2008; Farooq et al., 2019) result in POD, CAT, OXD, and SOD activities (Huang Y. et al., 2016; Tang et al., 2022), whereas Co_3O_4 NPs exhibit semiconducting attributes marked by Co^{3+} - Co^{2+} hopping (Cheng et al., 1998; Pham et al., 2016; Ibrahim et al., 2018), enabling intrinsic POD and CAT activities (Mu et al., 2012; Mu et al., 2014; Li et al., 2018; Wang et al., 2018). Other NPs like $\alpha\text{-}FeSe$, and Cu_2O/CuO , known for their superconductivity (Ito et al., 1991; Hsu et al., 2008; Sidorov et al., 2011; Lai et al., 2015), also demonstrate intrinsic POD activity (Dutta et al., 2012a; Dutta et al., 2012b; Dutta et al., 2013; Liu T. et al., 2020; Jiang et al., 2021; Zhu et al., 2021). NPs

with lower bandgaps and electron hopping, such as titanium dioxide (TiO_2) (Setvin et al., 2014; Xu Z. F. et al., 2022), manganese selenide (MnSe) (Liu et al., 2023), and molybdenum selenide (MoSe_2) (Suri and Patel, 2017), also display intrinsic POD activity (Zhang et al., 2013; Qiao et al., 2014; Wu et al., 2017). An interesting case are nanocrystalline cerium oxide NPs (ceria, CeO_2), which, due to their high electron conductivity and hopping attributes (Tuller and Nowick, 1977; Kim and Maier, 2002), can directly convert Ce^{4+} to Ce^{3+} due to oxygen vacancies (Esch et al., 2005). This enables ceria NPs to function like oxidoreductases (POD, CAT, OXD, SOD) (Yang et al., 2016a; Montini et al., 2016; Chen et al., 2022; Ma et al., 2022; Xiao et al., 2022), but also like nucleases, phosphatases and photolyases (Zhu et al., 2008; Dhall et al., 2017; Tan et al., 2020a; Tan et al., 2020b)

This review aims to deepen our understanding of the processes that led to the emergence of life on Earth. By bridging the disciplines of inorganic chemistry and biology, we highlight the potential role of inorganic nano-materials in catalyzing complex enzyme-like pre-biotic chemical processes. We propose that these inorganic NPs could have served as the initial biocatalysts for the emergence of the first life forms and subsequent evolutionary processes. This hypothesis challenges established concepts in modern biology, chemistry, and science as a whole. In **Section 2** and **Section 3**, we highlight how the metallic architecture of NPs and their electron hopping characteristics contribute to enzyme-like activity. The physical properties related to ET are foundational to the activity of NPs and may have been crucial in the emergence of life. In **Section 4** we will discuss the relevance of such catalytically active NPs in a biological context.

2 Architectural changes of iron nanocolloids and their impact on catalytic activity

Iron oxide systems with CAT-like activity are excellent model systems to illustrate the connection between their architecture and activity. The CAT-like activity of ten synthetic oxide colloids, i.e., 2-line ferrihydrite (2L-Fht, $\text{Fe}_5\text{HO}_8\cdot 4\text{H}_2\text{O}$), 6-line ferrihydrite (6L-Fht, $\text{Fe}_5\text{HO}_8\cdot 4\text{H}_2\text{O}$), goethite (Goe, $\alpha\text{-FeOOH}$), akageneite (Aka, $\beta\text{-FeOOH}$), lepidocrocite (Lep, $\gamma\text{-FeOOH}$), feroxyhyte (Foh, $\delta'\text{-FeOOH}$), Hem ($\alpha\text{-Fe}_2\text{O}_3$), Mah ($\gamma\text{-Fe}_2\text{O}_3$), Mag (Fe_3O_4) and schwertmannite (Sch, $\text{Fe}_8\text{O}_8(\text{OH})_6\text{SO}_4$) (**Figure 1A**) were compared by monitoring the molecular oxygen they produce in an aqueous H_2O_2 solution over time (**Figure 1B**) (Zhang R. et al., 2021). The activity was found to depend on the number of hydroxyl groups on the surface of the iron oxide colloids (**Figure 1C**) (Zhang R. et al., 2021).

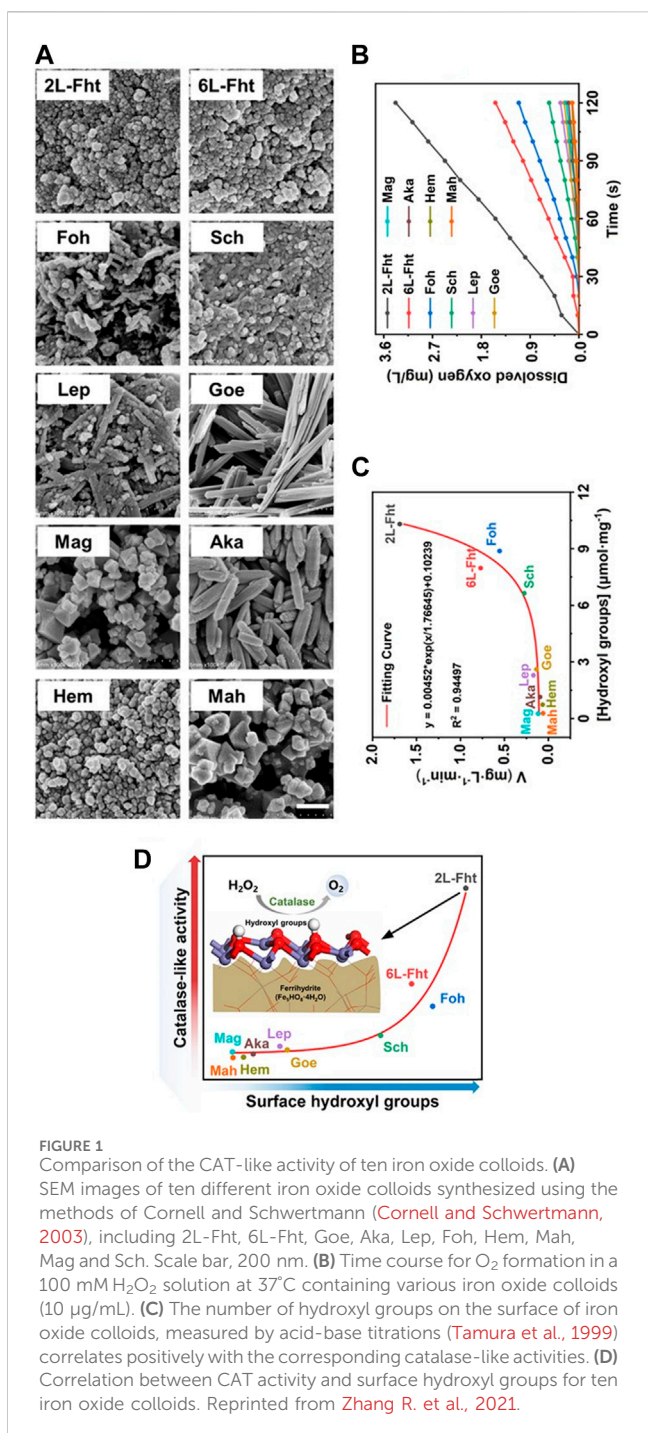
Iron oxide colloids that have hydroxyl groups in their core structures (2L-Fht, 6L-Fht, Foh) all have significant CAT-like activity, while those that do not (e.g., Hem, Mag and Mah) have no or little activity (**Figure 1D**) (Zhang R. et al., 2021). Some iron oxide colloids exhibit catalytic promiscuity by having not only CAT-like, but also OXD- and SOD-like activities, all associated with hydrogen peroxide and free oxygen radicals (Chen et al., 2012; Guo and Guo, 2019; Qin et al., 2019; Gu Y. et al., 2020; Chong et al., 2021; Zhao et al., 2021; Xu D. et al., 2022; Gao, 2022). Ferrihydrites, in particular, have high intrinsic CAT-like activity but low intrinsic POD-like activity due to the higher abundance of hydroxyl groups in

their crystalline structure compared to other iron oxide colloids (Zhang R. et al., 2021).

Iron oxide nanocolloids¹ with intrinsic oxidoreductase activity are not limited to synthetic compounds. Inherent oxidoreductase activity has also been observed in Mag from magnetotactic bacteria (MTB) after removing the magnetosome protein membrane (Hu et al., 2010; Li et al., 2015). Biogenic iron oxide colloids from *Burkholderia* sp. YN01v (Fe_3O_4) (Pan et al., 2015; Pan et al., 2019), *Comamonas testosterone* ($\text{Fe}_{1.44}\text{O}_{0.32}(\text{OH})_{3.86}$) (Ahmed et al., 2019) and *Acinetobacter* strains ($\text{Fe}_{0.96}\text{O}_{0.88}(\text{OH})_{1.12}$) (Abagana et al., 2022) also exhibit intrinsic POD (Pan et al., 2015; Ahmed et al., 2019; Abagana et al., 2022), SOD (Pan et al., 2019) and CAT-like (Pan et al., 2019) activities. The mineral core of ferritin also exhibits POD activity that follows Michaelis-Menten-type kinetics for the oxidation of TMB, OPD and N, N-diethyl-1,4-phenylenediamine (DPD) (Arapova et al., 1999; Tang et al., 2011), as well as SOD activity (Zhang J. et al., 2021). A recent study also shows that the iron cores of various ferritins (Archaea: *Pyrococcus furiosus*, *Pyrococcus yayanosii*, and *Sulfolobus solfataricus*; Bacteria: *Escherichia coli*; Eukaryotes: *Homo sapiens*) exhibit oxidoreductase activity (POD, CAT, OXD, and SOD) after protein removal (Ma et al., 2024). This activity is attributed to their metal structure rather than the organic compounds in ferritins, particularly the amino acid sequences (Ma et al., 2024).

Iron sulfide nanocolloids have also been reported to have intrinsic oxidoreductase activity, similar to biological oxidoreductases that contain iron-sulfur (Fe-S) clusters, such as alkyl hydroperoxide reductase (Poole, 1996; Hall et al., 2011), disulfide bond oxidoreductase D, rubredoxin or Rieske dioxygenases (Katzen and Beckwith, 2000; Krupp et al., 2001). Furthermore, Fe-S suspensions were shown to catalyze the oxidation of POD substrates such as TMB in the presence of peroxide (Dai et al., 2009; Dutta et al., 2012b). The apparent K_m values of Fe_7S_8 nanowires for H_2O_2 and TMB are 0.895 mM and 0.548 mM, respectively, and the corresponding K_m values of HRP

¹ The term “nanocolloids” is used here to highlight the importance of size (<100 nm) and high surface area-to-volume ratio in the enzyme-like activity of inorganic NPs. It is important to note that not all fine-grained mineral particles (colloids) exhibit the same enzyme-like activity. While the term “nanozyme” has become popular for describing NPs with enzyme-like activities, it is essential to understand its historical development. Initially, the term “nanozyme” referred to triazacyclonane/ Zn^{2+} -functionalized gold NPs as RNase mimics (Manea, F., Houillon, F.B., Pasquato, L., and Scrimin, P. 2004. Nanozymes: Gold-nanoparticle-based transphosphorylation catalysts. *Angew. Chem. Int. Ed.* 43, 6,165–6,169) Later, it was expanded to include nanomaterials with enzyme-like characteristics (Wei, H., and Wang, E. 2013. Nanomaterials with enzyme-like characteristics (nanozymes): Next-generation artificial enzymes. *Chem Soc Rev* 42, 6060–6093). Our review focuses on natural NPs, historically referred to as colloids, which encompass particles ranging from micro-to nanometer-sized dimensions. By using the term “nanocolloids,” we aim to underscore the natural origin and properties of NPs, distinguishing them from the artificial or engineered NPs often associated with nanozymes.



are 0.834 and 3.386 mM, demonstrating again that simple inorganic structures can have substrate affinities that are at least as strong as those of biological representatives (Yao et al., 2013). Greigite nanocolloids ($Fe^{2+}Fe^{3+}_2S_4$, structural equivalents of Mag) also possess POD-like activity with a high affinity for H_2O_2 (Ding et al., 2016; Liu W. et al., 2020). In addition, a nano-colloidal pyrite compound (“pyrite nanozyme”) has recently been shown to have a 3300-fold higher affinity for H_2O_2 than Mag, with a more than 4000-fold higher catalytic activity (Meng et al., 2021). It has also been shown that iron polysulfide particles possess POD, CAT

and intrinsic glutathione oxidase (GSH-OXD)-like activity (Xu et al., 2018; Cao et al., 2023). These iron sulfide colloids can decompose H_2O_2 into free radicals and O_2 , promoting the release of polysulfides. Similar to CAT-, OXD- or SOD-catalyzed reactions various reactive oxygen species (such as hydroxyl ($\cdot OH$), hydrogen peroxide (H_2O_2), superoxide ($\cdot O_2^{\bullet}$) and singlet oxygen ($\cdot O_2$) are formed in reactions catalyzed by these colloids (Kantar et al., 2019; Nie et al., 2019; Ding W. et al., 2020; Agnihotri et al., 2020; Wang et al., 2020; Huang et al., 2021; Ren et al., 2021; Song et al., 2022). Since most of these ROS trigger cytotoxic effects, metal sulfide nanocolloids may provide a novel therapeutic function (Yuan et al., 2020; Shan et al., 2022).

In addition to size, shape and surface area, recent data indicate that the metal architecture of nanocolloids, including iron oxides, plays a crucial role in enzyme-like activities associated with ET functions (Liu et al., 2011; Puvvada et al., 2012; Cheng et al., 2014; Mu et al., 2014; Peng et al., 2015; Ghosh et al., 2018; Xu Z. et al., 2021; Zhang R. et al., 2021; Jiang et al., 2021; Chen et al., 2022; Singh et al., 2022; Zhang et al., 2022). In general, the metal architecture of iron oxides is determined by their ferric-ferrous composition (e.g., Fe^{3+}/Fe total) and the hydroxylation ratio (OH/Fe total), as illustrated in Figure 2A (Cornell and Schwertmann, 2003; Jolivet et al., 2006; Jolivet, 2019). As an example, Figure 2B shows the basic structural unit of 2L-Fht/6L-Fht and other iron oxide colloids in a Back-Figges δ -Keggin cluster (Fe_{13}), which contains 13 iron and 40 oxygen atoms (Michel et al., 2007; Michel et al., 2010). The central, tetrahedrally coordinated Fe is connected to 12 peripheral, octahedrally coordinated Fe atoms arranged in edge-sharing groups of three by oxo bridges. In this arrangement, iron oxide nanocolloids between 2 and 6 nm in size can be viewed as a three-dimensional packing of such clusters. Adjacent clusters are connected by a typical pair of edges, corners or faces, or by a combination-shared octahedra, forming oxo bridges in the bare cluster (Figure 2C) (Michel et al., 2007). The Fe-Fe distance depends on the architecture, with the corner-sharing arrangement having the longest (3.39–3.70 Å) and the face-sharing arrangement having the shortest distance (2.88 Å; Figure 2D) (Manceau and Combes, 1988; Cornell and Schwertmann, 2003).

The metal architecture of iron oxide colloids is susceptible to changes in the environment, including exposure to oxygen, reactive oxygen species, light, nitrate, ferrous or ferric irons, and phosphorus (Usman et al., 2018; Kappler et al., 2021). For instance, solar irradiation promotes a photo-oxidation process, even in the absence of oxygen (Braterman et al., 1983), triggering the transformation of Fht into Goe (Shu et al., 2019). Superoxide radicals were suggested to act as primary oxidants for Fe^{2+} under acidic conditions promoting the formation of iron oxide colloids (Shu et al., 2022). It has also been demonstrated that ferric oxyhydroxides such as Fht, Lep or Goe can be transformed into Mag when reacted with ferrous iron under alkaline conditions over time (Usman et al., 2012). Mag colloids are capable of converting into Mah, not only via oxidation by oxygen, various ions and/or ETs through the solid-solution interface (Jolivet and Tronc, 1988), but also through interaction with bacteria (Auffan et al., 2008). A similar transformation of the iron architecture has also been observed when Hem interacts with the iron-reducing bacterial strain *Shewanella oneidensis* MR-1 (Luo et al., 2017). Raman spectroscopy and analysis

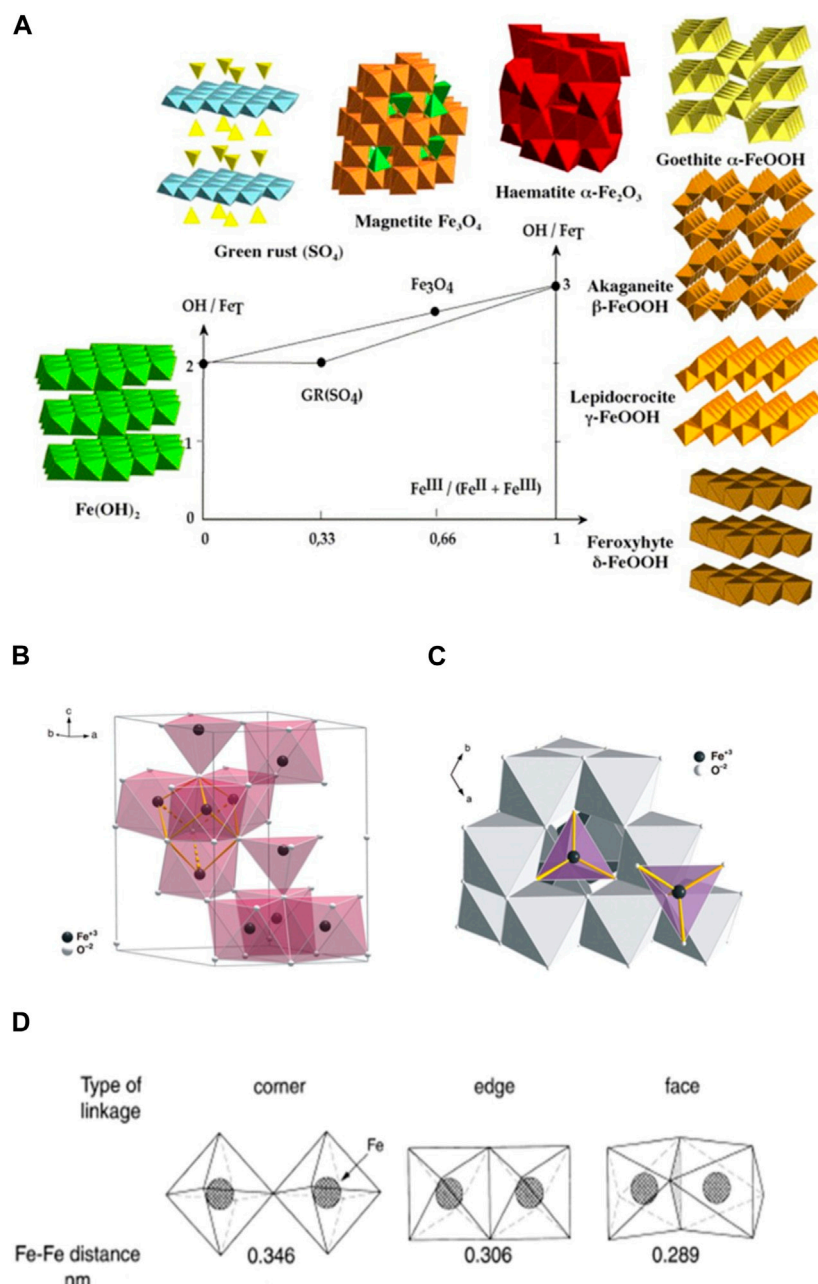


FIGURE 2

Metal architecture of iron oxide colloids. (A) Main structure types of iron oxides (Jolivet et al., 2006) (reprinted with permission from Dr. Jolivet). (B) The Back-Figgis δ -Keggin Fe_{13} cluster. Polyhedral representation of the ideal ferrihydrite structure viewed along the c axis. The central FeO_4 tetrahedra are surrounded by 12 FeO_6 octahedra. (C) The basic structural motif consists of a central FeO_4 tetrahedron surrounded by 12 FeO_6 octahedra. The bonded atoms (yellow) define a cube-like moiety that connects the basic structural motifs of the model (reprinted from Michel et al., 2007, Copyright © 2007, AAAS). (D) The $\text{Fe}-\text{Fe}$ distance and linkage of octahedra in Fe^{3+} oxides (reprinted from Cornell and Scherstmann (2003). Copyright @ 2003 John Wiley and Sons).

of magnetic properties reveal that this bacterial strain can transform the crystalline structure of Hem colloids from a hexagonal to a cubic system through microbial, extracellular ET. This transformation can also be monitored using electron paramagnetic resonance (EPR) spectroscopy, which shows that changes in the crystalline structure of Fe^{2+} lead to the biotransformation of Hem into Mag (Luo et al., 2017).

The changes in the internal atomic structure of nanocolloids play an important role in their reactivity. For example, near-spherical Mag NPs with an average diameter of 10.16 ± 0.12 nm, gradually lose POD-like activity during their transformation from Mag to Mah. This transformation interferes with the rate of the ET at the surface of these nanocolloids (Figure 3) (Dong et al., 2022). The specific POD-like activity (a_{nano}) of Mag, Mah and Hem NPs

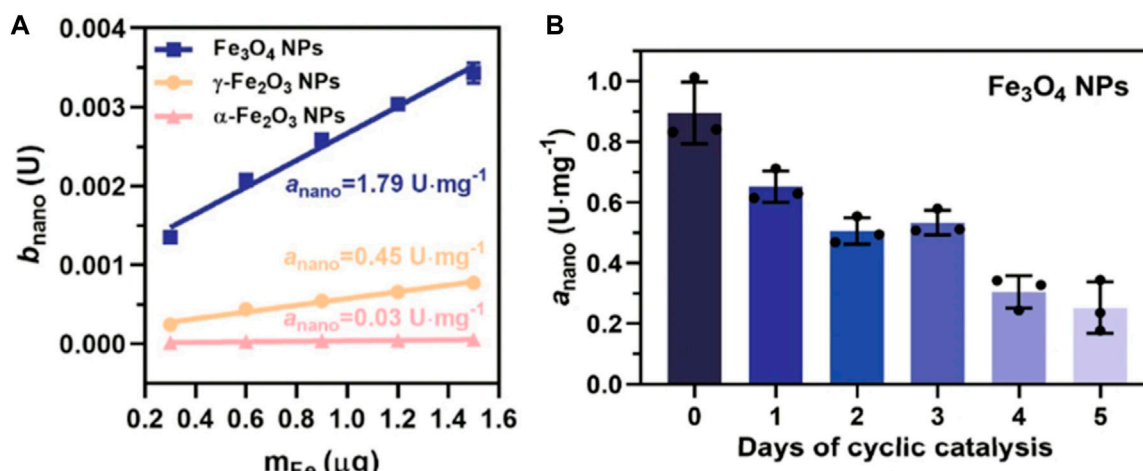


FIGURE 3

Schematic diagram of the catalytic mechanism of the activity of inorganic POD (Dong et al., 2022) (A) The specific POD-like activity (a_{nano}) of Mag (Fe_3O_4), Mah ($\gamma\text{-Fe}_2\text{O}_3$) and Hem ($\alpha\text{-Fe}_2\text{O}_3$), measured with TMB as colorimetric substrate. (B) Kinetic study of a_{nano} values of Fe_3O_4 NPs with the days of cyclic catalytic reaction. U is defined as 1 $\mu\text{mol}/\text{min}$ for enzyme activity. Error bars represent standard deviation from three independent measurements. Reprinted from Dong et al., 2022.

are 1.79, 0.45 and 0.03 Umg^{-1} , respectively (Figure 3A) (Dong et al., 2022). However, the values of a_{nano} of Mag significantly decrease over time (Figure 3B) (Dong et al., 2022). Changes in the metal architecture are not limited to the colloid surface as the interior Fe^{2+} of Mag NPs are also gradually oxidized during prolonged reaction times. As a result, the catalytic activity of recovered NPs also gradually decreases concomitantly with an increase in their oxidation state (Dong et al., 2022). It has been proposed that ET to the surface via $\text{Fe}^{2+}\text{-O-Fe}^{3+}$ chains may enable the regeneration of surface Fe^{2+} , thereby sustaining POD-like catalytic activity. The efficiency of this step has been proposed as the rate-limiting factor in NP-catalyzed reactions (Dong et al., 2022). Keep in mind that inorganic NP structures are not rigid and unchanging entities. Instead, they dynamically respond to a myriad of external influences, including both abiotic and biotic factors, as well as catalytic processing. These factors significantly impact the behavior of biocatalysts and have implications for the importance of metal center stabilization in the evolution of proteins.

3 Electron transfer mechanisms in inorganic iron oxide and iron sulfide nanocolloids

In the previous section we focused on the connection between architecture and catalytic activity and how NPs can change their architecture and hence also their activity. Here, we concentrate on the electronic properties of catalytically active colloids, their dependence on structure and their implications for catalysis or chemical transformations.

In inorganic colloids, the band gap (*i.e.*, the energy required to remove an electron from its valence shell) plays a significant role in ET processes and hence catalytic activity. The band gap is inherently related to the electron configuration, structural characteristics and charge ordering (*i.e.*, the long-range order of different metal

oxidation states within the crystal lattice of the colloids (Verwey, 1939)). A narrow band gap facilitates electron hopping, a phenomenon where electrons spontaneously move between localized states or sites within a material through a series of intermediate states. This efficient movement of electrons contributes to the material's catalytic activity by promoting effective ET processes.

On the other hand, proteins, DNA and RNA also exhibit electron hopping due to their own unique structural and chemical properties (Giese, 2018). The study of the connection between ET and conductivity at the molecular level, particularly the interplay between solid-state physics and bioinorganic chemistry, is an area of active research (Bostick et al., 2018; Mostajabi Sarhangi and Matyushov, 2023). The occurrence of electron hopping has been suggested for various iron oxide colloids, such as Mag (Skomurski et al., 2010), Fht (Alexandrov and Rosso, 2014), Goe (Zarzycki et al., 2015), green rust (Wander et al., 2007) and Hem (Jordanova et al., 2005; Kerisit and Rosso, 2006). Experimental observations have confirmed electron hopping on the surfaces of Fht (Katz et al., 2012), Hem (Carneiro et al., 2017; Husek et al., 2017), and Mah (Ibrahim et al., 2018).

The electrical conductivity of Mag nanocolloids, for instance, is affected by alternating current (AC) frequency and temperature, as shown in Figure 4A (Radoñ et al., 2018). Conductivity dispersion as a function of AC frequencies is closely related to both long-range (conduction mechanism associated with grain boundaries) and short-range mobility (conduction mechanism associated within grains; Figure 4B). The blue arrow represents the tunnelling of small polarons, the solid red arrow represents electron hopping, and the black arrow represents electrons moving between Fe^{2+} and Fe^{3+} ions in the crystal structure. At high temperatures and low frequencies, tunnelling of small polarons occurs, which is associated with the polarization of grain boundaries and manifests itself as long-range mobility (Figure 4B) (Radoñ et al., 2018).

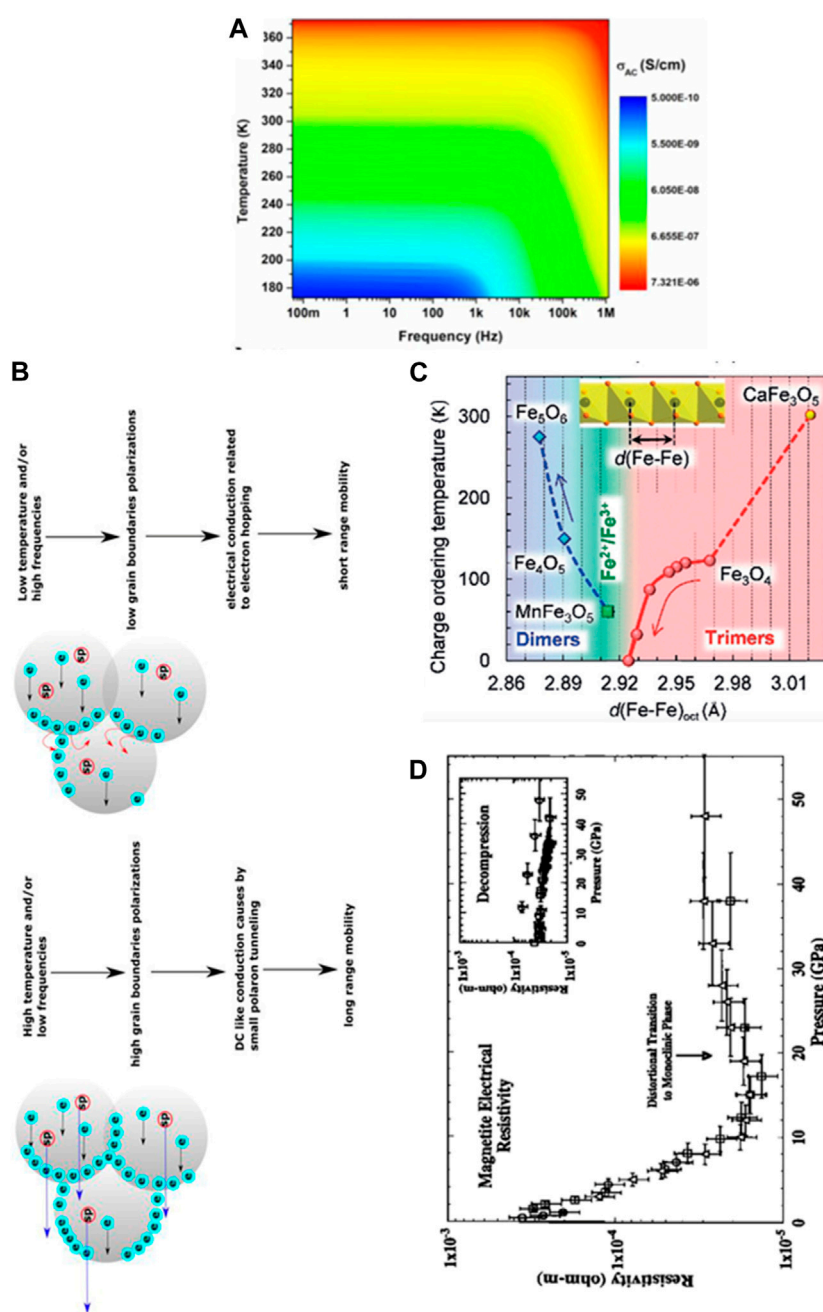


FIGURE 4

Structure and electrical characteristics of inorganic iron oxide colloids. (A) Surface plot of AC conductivity of Mag as a function of temperature and frequency. (B) Two conduction mechanisms in different temperature and frequency regions (Reprinted from Radoń et al., 2018). (C) Dependence of the charge-ordering transition temperature for Fe_5O_6 , Fe_4O_5 , MnFe_3O_5 , Fe_3O_4 , and CaFe_3O_5 on the minimal Fe–Fe distances in their octahedral iron chains (Reprinted from Ovsyannikov et al., 2020). (D) Response of electronic resistivity of Mag under different pressures (Reprinted with permission from Morris and Williams, 1997, Copyright © 1997, John Wiley and Sons).

Alterations in the Fe–Fe distance in the octahedral chains of various iron oxide colloids can also affect the ability of electrons to hop or tunnel between ions, leading to changes in charge ordering that relates to electrical conductivity (Todo et al., 2001; Senn et al., 2012; Ovsyannikov et al., 2016; Hong et al., 2018; Ovsyannikov et al., 2018; Cassidy et al., 2019; Ovsyannikov et al., 2020) (Figure 4C). Similar effects on electronic properties under pressure (causing

structural changes) have been reported for Mah, Hem and Foh NPs (Morris and Williams, 1997; Pasternak et al., 1999; Ohta et al., 2010; Ohta et al., 2012) (Figure 4D).

The electrical conductivity of iron oxide nanocolloids is also influenced by their concentration; specifically, in a Mag nanofluid with varying volume fractions, the electrical conductivity increases with increasing temperature and weight fraction (Jamilpanah et al.,

2017). At 25°C, the electrical conductivity of the base fluid increased from 0.39 $\mu\text{S cm}^{-1}$ to 2,419 $\mu\text{S cm}^{-1}$ for a loading of 4 vol% iron oxide, which corresponds to an anomalous enhancement of over 6,000 fold.

The ferrimagnetic iron sulfide greigite (Fe_3S_4) has an inverse spinel structure, consisting of both Fe^{2+} and Fe^{3+} centers in a 1:2 ratio. The spin magnetic moments of the Fe cations in the tetrahedral sites are oriented in the opposite direction to those in the octahedral sites (anti-ferromagnetic coupling), resulting in a net magnetization (Devey et al., 2009; Patrick et al., 2017). Both metal sites have high-spin quantum numbers, and the mineral is a half-metal with an S vacancy structure and a magnetic moment of <4.0 μB per formula unit (Li et al., 2014) (Figure 5A). Fe^{2+} - Fe^{3+} electron hopping occurs at the octahedral sites. When comparing the properties of Fe_3S_4 and Fe_3O_4 , the mean charges for octahedral Fe are 1.0 e^- and 1.7 e^- , respectively, while for tetrahedral Fe, they are 1.1 e^- and 1.8 e^- , respectively. The value of magnetization of saturation (M_s) in sulfides is slightly less than that of oxides (Roldan et al., 2013) and the resistivity of sulfides is also less than that of oxides (Figure 5B) (Li et al., 2014).

Another iron sulfide example is pyrrhotite (Fe_{1-x}S ; with x varying between 0 and 0.13), which has a hexagonal crystal structure, where the metal ions are in an octahedral coordination environment and the anions in a trigonal prismatic arrangement. A crucial feature of this structure is the ability to omit metal atoms up to one in every eight (1/8), thereby creating iron vacancies. One such structure is pyrrhotite-4C (Fe_7S_8) (Sakkopoulos et al., 1984; Sagnotti, 2007). The Fe deficiency affects both the crystallographic and magnetic structures. The ordering of the Fe vacancies leads to an alternating arrangement of partially vacant and fully filled Fe layers, the hexagonal structure distorts to monoclinic and the magnetic ordering turns from antiferromagnetic to ferrimagnetic (Takele and Hearne, 1999; Roberts et al., 2018; Živković et al., 2021). Like in iron oxides, the structures of iron sulfide colloids also change with pressure (Takele and Hearne, 1999) or temperature (Roberts et al., 2018). The highly symmetrical structure of FeS results in an overall net zero magnetic moment across the unit cell. In contrast, the low symmetry structure of Fe_7S_8 exhibits ferrimagnetism due to the uncompensated magnetic moment in the iron-vacancy-rich layers. The vacancy-free sample ($x = 0$, troilite) has a metallic state in resistance and exhibiting superconductivity below 4.5 K (Lai et al., 2015). In contrast, for the samples with Fe vacancies ($x \geq 0.05$), no superconductivity is observed, and the samples exhibit semiconducting behavior (Guo et al., 2017; Kuhn et al., 2017). Delocalized electrons in ultrathin Fe_7S_8 nanosheets facilitate ET as the d orbitals of Fe^{2+} and Fe^{3+} overlap. This electronic property is critical for its utilization as a catalyst, making ultrathin pyrrhotite nanosheets a very efficient Fe-based electrocatalysts for water oxidation (Chen et al., 2017).

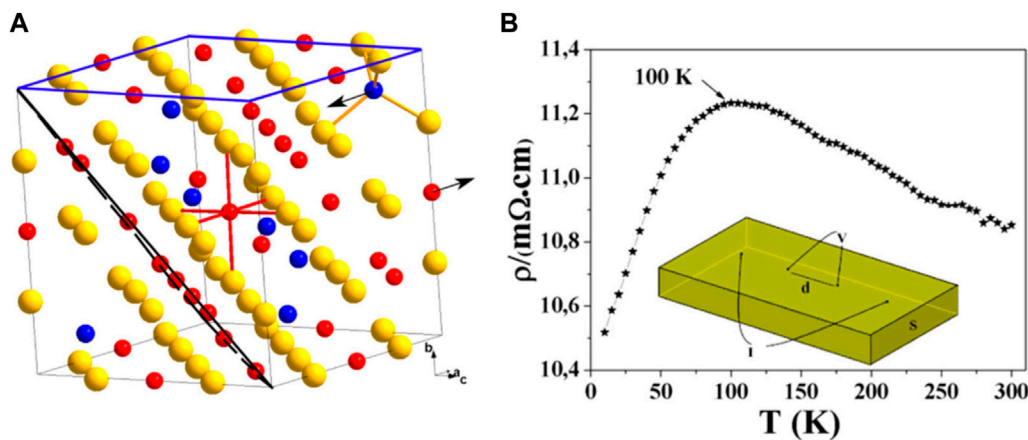
In summary, the crystal structures of iron oxides and sulfides significantly influences their electrical properties, which are determined by the coordination of iron with oxygen or sulfur and the corresponding electronic configurations. The electron configuration and coordination of iron with oxygen or sulfur are crucial factors in determining the metal architecture of colloids, which contributes to their unique properties, including size and shape (Wu et al., 1997; Cornell and Schwertmann, 2003; Grau-

Crespo et al., 2010; Yu et al., 2012; Erlebach et al., 2015; Noh et al., 2015; Huang X. et al., 2016; Li et al., 2017; Jian et al., 2019; Paidi et al., 2021). Iron oxides and sulfides exhibit semiconductor behavior with low band gaps, facilitating ET. The non-uniform coordination of Fe 3d electrons with oxygen or sulfur atoms yields a material that can induce intrinsic spontaneous electron hopping at non-uniform octahedral surface sites.

4 The relevance of inorganic oxidoreductase activity in biological systems

Iron oxide and sulfide nanocolloids are abundant on Earth and can be found in diverse habitats, including soils, water, rocks and living organisms (Cornell and Schwertmann, 2003; Jolivet et al., 2006; Rickard and Luther, 2007; Sagnotti, 2007; Navrotsky et al., 2008; Konishi et al., 2012; Guo and Barnard, 2013; Posth et al., 2014; Maher, 2016; Claudio et al., 2017; Yuan et al., 2020; Huang, 2022b). These encompass diverse environments such as high pH hydrothermal vents (Lough et al., 2019; Yücel et al., 2021), ice sheets (Hawkings et al., 2014), fly ash and street dust (Yang et al., 2016b; Gonet and Maher, 2019). Remarkably, they are also found in magnetosomes from Magnetotactic Bacteria (MTB) (Pósfai et al., 2013; Uebe and Schüler, 2016; Goswami et al., 2022), as well as in other biogenic iron minerals (Posth et al., 2014). These nanocolloids form through various mechanisms (Guo and Barnard, 2013), resulting in a range of sizes, shapes, and structures (Xie et al., 2018). Iron sulfide nanocolloids are prevalent in hydrothermal vent plumes (Findlay et al., 2019; Yücel et al., 2021) and can be found in many marine sediments (Rickard and Luther, 2007; Gu X. et al., 2020; Subramani et al., 2020). Geological evidence indicates that secondary pyrrhotite, pyrite, greigite, mackinawite and green rust (fougerite) may have existed as nanocolloids during the Hadean and early Archean era, a time period that predates and overlaps with the emergence of proteins and primitive life forms (Holland, 2007; Raiswell and Canfield, 2012; Bekker et al., 2013; Catling, 2013; Halevy et al., 2017; Goswami et al., 2022). Notably, simulations conducted in origin-of-life reactors produced pyrrhotite, pyrite and mackinawite (Herschy et al., 2014; White et al., 2015; White et al., 2020). Fe_2O_3 NPs obtained from PVC dichlorination residues and iron chips treated with subcritical water exhibit inherent peroxidase-like properties (Qi et al., 2023). It is anticipated that any iron oxide NPs with the same metal architecture continue to function as biocatalysts, a realization yet to be fully acknowledged.

During the Archean era, the primitive atmosphere was mainly composed of nitrogen, carbon monoxide, carbon dioxide and methane (Kasting et al., 1984; Lyons et al., 2014) but also potentially low levels of O_2 and H_2O_2 (Zuo and Deng, 1999; Borda et al., 2001; Lee et al., 2019; He et al., 2021; Jenkins et al., 2021; Stone et al., 2022). The oceans contained Fe^{2+} and transition metal oxide, sulfide and potentially selenide nanocolloids (Braterman et al., 1983; Holland, 2007; Nitschke and Russell, 2009; Bekker et al., 2013; Shu et al., 2019; Shu et al., 2022). In order to broadly address the roles of metal nano-to sub-micro-sized catalysts on life and the habitability of Earth, we need to consider the basic requirements for life, i.e., all cells need a source of energy and are composed of water, organic carbon molecules and essential

**FIGURE 5**

Structure and electronic properties of an Fe_3S_4 colloid. **(A)** Crystal structure of Fe_3S_4 with the (001) and (111) planes outlined in blue and black, respectively. Sulfur atoms (yellow spheres) form a cubic close-packed lattice: 1/8 of the tetrahedral A sites are occupied by Fe^{3+} (blue spheres) and 1/2 of the octahedral B sites are equally occupied by Fe^{2+} and Fe^{3+} (red spheres). The magnetic moments on the A and B sites are antiparallel and aligned along the [100] crystallographic axis (indicated by arrows). **(B)** Resistivity of Fe_3S_4 between 5 K and 300 K, and the corresponding contact geometry (inset).

Reprinted with permission from Li et al., 2014, Copyright © 2014, ACS.

elements (hydrogen, oxygen, nitrogen, phosphorus, and sulfur). The occurrence of complex organic carbon molecules and essential elements in the materials that formed the proto solar system cloud suggests that these materials, and possibly mineral catalysts were ubiquitous. Endogenous sources of organic carbon included the primordial, slightly reducing atmosphere (Miller, 1953; Johnson et al., 2008) and active hydrothermal systems producing organic carbon via Fischer Tropsch synthesis, e.g., the Rainbow ultramafic hydrothermal system on the Mid Atlantic Ridge (Russell et al., 2010). A significant number of organic molecules (and other volatiles, such as water) were also delivered from extraterrestrial sources, e.g., carbonaceous chondrites, containing up to 5% organic carbon (Sephton and Botta, 2008; Potiszi et al., 2023). Habitable conditions are defined by the sum of the physical and chemical conditions that support the presence of liquid water at the surface of a planetary body. Under standard (Earth) temperature and pressure, the occurrence of liquid water and catalytic activity could have occurred over a broad range of temperatures (-15°C – 100°C) and salinity (freshwater to saturated brines), conditions that are considered to be extreme on Earth today. An origin of life under these extreme conditions is thought to be aligned with the Archaeal domain (Woese et al., 1990), which is dominated by prokaryotes that thrive in anaerobic (methanogen), thermophilic (high temperature) and halophilic (salt loving) extreme environmental conditions, common on early Earth. Anaerobic (reducing) mineral catalysts, e.g., iron sulfides, would have affected the geochemistry of this early Earth, producing substrates for early life from the late heavy bombardment ~3.9 billion years ago (Gomes et al., 2005) and continuing through the origin of life era, about 3.5 billion years ago (Westall and Southam, 2006), until the Great Oxidation Event (GOE) beginning from ~ 2.5 billion years ago. During this time, the Earth possessed an anaerobic, habitable environment with < 0.2% of the present atmospheric oxygenic levels (Catling and Claire, 2005) and that was significantly hotter (Knauth and Lowe, 2003; Cavalazzi et al., 2021) and more volcanically/hydrothermally active (Hofmann

and Bolhar, 2007) than most contemporary systems. The low levels of reactive oxygen produced by photolysis (Kasting, 1993) relative to the abundance of reduced chemical species would have resulted in a correspondingly reducing chemistry for the hydrosphere and lithosphere, though some transient metal oxides, i.e., metal oxide colloids, may have been formed and been ‘active’ in this system. From the GOE forward, Earth has had variable, but more oxidizing conditions, increasing the diversity of catalytic nanomaterials, e.g., partially oxidizing (such as Mag) to fully oxidizing materials (such as 2L-Fht or 6L-Fht), as well as the ‘earlier’ reducing mineral catalysts.

Ever since the GOE, the presence of hydrogen peroxide and free radicals in the environment has been a challenge for living cells, in particularly anaerobic bacteria, which do not have efficient enzymatic detoxification strategies (Dröge, 2002; Halliwell, 2006; Ślesak et al., 2007; Sies, 2017; Taverne et al., 2018; Taverne et al., 2020). ROS, such as hydrogen peroxide, are byproducts of normal metabolic processes in cells and can cause oxidative damage to cellular components such as DNA, proteins and lipids. The Snowball Earth and GOE periods may have contributed to an increase in atmospheric hydrogen peroxide levels, potentially leading to detrimental effects such as mutations, cell death and other adverse impacts on organism survival and evolution (Liang et al., 2006). It has been speculated that essential enzymes like SOD, CAT and POD may have existed prior to the GOE (Castresana et al., 1994; Zelko et al., 2002; Ślesak et al., 2012; Zámocký et al., 2012; Inupakutika et al., 2016; Ślesak et al., 2016; Case, 2017; Olson et al., 2017). Furthermore, their activities may have been complemented/augmented by iron oxide and sulfide nanocolloids, thus mitigating the detrimental effects of ROSs (Huang, 2018; Huang, 2022a). Such activities are found in all domains of life, including obligate anaerobes, suggesting that the need for such protection prevailed even in anaerobic environments (Runnegar, 1991; Castresana and Saraste, 1995; Lenton, 2003; Neubeck and Freund, 2020). These suggestions are consistent with the hypothesis that inorganic iron oxide or sulfide colloids with intrinsic

oxidoreductase activity and/or which promote spontaneous electron hopping may have been crucial to establish and enhance biological reaction rates at the onset of biological evolution. Remarkably, iron oxide nanocolloids, such as Mag and ferrihydrite, can directly cross lipid bilayers and enter the cytoplasm and other cellular compartments of eukaryotic cells without damaging the plasma membrane (Zanella et al., 2017; Chilom et al., 2020).

As described above, some microorganisms are able to trigger architectural changes of iron colloids, especially the nanocolloids and consequently can also alter their catalytic activity (e.g., *E. coli* or *S. oneidensis* MR-1 (Luo et al., 2017)). Another example is *Trichoderma guizhouense*; incubation of Mag nanocolloids with this fungus leads to a significant increase in their POD-like activity (~2.4-fold increase) (Chi et al., 2021). These observations demonstrate that nature is not only able to utilize inorganic colloids but to also optimize their oxidoreductase activity through modifications of their metal architecture. Further, recent research has demonstrated that the ET rate of inorganic iron oxide NPs can also be augmented by small molecules such as amino acids or nucleotides (Fan et al., 2017; Niu et al., 2018; Wu W. et al., 2019; Chen J. et al., 2020; Han et al., 2020; Niu et al., 2020; Vallabani et al., 2020; Xu W. et al., 2021; Geng et al., 2021; Han et al., 2021; Sun et al., 2021; Wang et al., 2023). It is widely accepted that primitive precursors of these molecules emerged early during Earth's prebiotic evolution (Miller, 1953; OrÓ, 1961; Ferus et al., 2017; Frenkel-Pinter et al., 2022), contributing to the development of life, including the formation of proteins, DNA and RNA. For instance, the complexation of Mag NPs with the amino acid histidine (His) improves their K_m for H_2O_2 over ten-fold (from 459 mM to 38 mM) and increases their catalytic efficiency (k_{cat}/K_m) up to 20-fold (from $0.68 \times 10^6 \text{ s}^{-1}\text{M}^{-1}$ to $14.2 \times 10^6 \text{ s}^{-1}\text{M}^{-1}$) (Fan et al., 2017). For comparison, the corresponding values for the enzyme HRP are 10.4 mM and $0.29 \times 10^6 \text{ s}^{-1}\text{M}^{-1}$ (Fan et al., 2017). The addition of organic functional groups, such as amino acids or nucleotides, to inorganic oxidoreductases likely played a vital role in stabilizing the structure of the early catalysts during evolution (Huang, 2022a), while also promoting electron tunneling (*via* super-exchange) and hopping (Halpern and Orgel, 1960; Hopfield, 1974; Marcus and Sutin, 1985; Warren et al., 2012; Gray and Winkler, 2015; 2021). Notably, electrons can tunnel through peptides in microseconds over distances of 15–20 Å, a phenomenon assisted by aromatic side chains of amino acids such as tryptophan (Trp) and tyrosine (Tyr) (Gray and Winkler, 2021).

In the study of ET in proteins, attention is given to factors such as the amino acid composition, overall fold and hydrogen bonds (Dixon and Lipscomb, 1976; Dwyer, 2006; Warren et al., 2012; Berstis et al., 2015; Gray and Winkler, 2015; Sepunaru et al., 2015; Gray and Winkler, 2021). Similarly, evolutionary studies of metalloenzymes have mostly focused on their protein folds (Grishin, 2001; Raanan et al., 2020), and less so on their metal centers (Holm et al., 1996; Drennan and Peters, 2003). Recently, it was proposed that metalloenzymes, including ribozymes (Pyle, 1993), may be considered as functionalized nanomaterials, in which the metal architecture serves as an active center that has been stabilized over time by amino acids and nucleic acids (Huang, 2022a). This line of thought is supported by the fact that certain inorganic colloids exhibit enzyme-like properties and with similar metal architectures as the active sites of enzymes such as POD, OXD,

CAT or SOD, but also purple acid phosphatase (Mitić et al., 2006; Huang and Zhang, 2007; 2012; Schenck et al., 2013; Huang, 2018; 2019), haloperoxidase (André et al., 2011; Natalio et al., 2012; Leblanc et al., 2015; Chen, 2022) and sulfite-oxidizing enzymes (Hille et al., 2014; Ragg et al., 2014; Kappler and Enemark, 2015). It is important to note that metalloenzymes have highly complex and fine-tuned structures that have evolved over time, incorporating both a metal center and specific amino acid side chains that contribute to their fold, tertiary/quaternary structures, as well as their ability to confer catalytic activity.

Another poignant example that illustrates the evolution of a metalloenzyme starting from an inorganic core is ferredoxin, an Fe-S-containing protein that was identified as an essential component of photosynthesis well before its amino acid sequence was known (Eck and Dayhoff, 1966). Indeed, Fe-S clusters were present in the last universal common ancestor (LUCA) of life on Earth, where they may have been used for various purposes, including ET and redox reactions (Weiss et al., 2016). This hypothesis is supported by research on hydrothermal vents that mimic conditions that may have been present at the onset of living organisms (Baross and Hoffman, 1985; Russell and Hall, 1997; Nitschke and Russell, 2009). The Fe-S clusters in proteins exhibit considerable similarity to various iron sulfides (Zhao et al., 2020; McGuinness et al., 2022). Relevant examples include eukaryotic ferredoxins and Rieske proteins that contain a Fe-S cluster with two Fe and two S atoms forming a 2Fe-2S diamond (Holden et al., 1994; Gurbel et al., 1996), while higher potential iron-sulfur proteins and iron regulatory proteins (IRPs) use four Fe and four S atoms to form a cubic 4Fe-4S cluster (Breiter et al., 1991; Solomon et al., 2000; Dupuy et al., 2006; Imlay, 2006). Rubredoxin, on the other hand, possesses a single iron atom coordinated by four equidistant sulfur atoms, forming a 1Fe-4S tetrahedron (Adman et al., 1991; Liu et al., 2015). Furthermore, although rare, 3Fe-3S (Bruschi and Guerlesquin, 1988) and 6Fe-6S clusters (Stokkermans et al., 1992) are also observed, demonstrating the architectural diversity of iron sulfide minerals. How these different clusters evolved in protein environments remains obscure. However, it is worth noting that iron sulfides with a single iron atom coordinated by four equidistant sulfur atoms exhibit superconductivity (Lai et al., 2015; Guo et al., 2017; Kuhn et al., 2017) and high inorganic oxidoreductase activity (Dai et al., 2009; Dutta et al., 2012b; Yao et al., 2013; Ding et al., 2016; Xu et al., 2018), suggesting that they may have played important roles in the biochemistry of LUCA and thus the evolution of FeS-containing proteins.

The catalytic activity of cubane-type Fe_4S_4 clusters in metalloproteins like biotin synthase (Reyda et al., 2009), aconitase (Castro et al., 2019), and (E)-4-hydroxy-3-methylbut-2-enyl pyrophosphate reductase (IspH) (Span et al., 2012), as well as in synthetic M_4S_4 clusters for various reactions, illustrates their possible role in the emergence of life and the formation of organic compounds from inorganic precursors (Seino and Hidai, 2011). Recent studies show that Fe-S clusters with low-valent Fe^{1+} centers can adopt a wide range of electronic configurations, crucial for their catalytic activity (Brown et al., 2022). CO binding to a synthetic $[\text{Fe}_4\text{S}_4]^{10-}$ cluster with N-heterocyclic carbene ligands triggers the generation of Fe^{1+} centers through intracluster ET, demonstrating the Fe-S clusters' ability to facilitate ET in redox

reactions. CO binding to an $[Fe_4S_4]^{+}$ cluster induces electron delocalization with a neighboring Fe site, resulting in a mixed-valent $Fe^{1.5+}Fe^{2.5+}$ pair, thus enabling the activation of C–O bonds without highly negative redox states (Brown et al., 2022). Metalloproteins with Fe_4S_4 clusters catalyze CO and CO_2 reduction to hydrocarbons (alkanes/alkenes) (Lee et al., 2010; Rebelein et al., 2015; Waser et al., 2023), significant in context of early Earth's life origins.

Pyruvate is a central metabolite in Archaea, Bacteria and Eukarya kingdoms, where iron-sulfur enzymes connect pyruvate to carbon fixation pathways and thioester biochemistry (De Duve, 1991; Berg et al., 2010). The $FeS/S/FeS_2$ system catalyzes hydroxyl acids and keto acids interconversion (Wang et al., 2011). Recent studies show natural iron sulfide pyrrhotite acting as an oxidoreductase catalyst in pyruvic acid to lactic acid conversion (De Aldecoa et al., 2013) and CO_2 reduction (Mitchell et al., 2021). Although these studies lack detailed kinetic data for the NPs' inorganic oxidoreductase activity, they align with Wächtershäuser's mineral surface study focusing on the iron-sulfur world and its relevance to evolutionary biochemistry (Wächtershäuser, 1988, 1990, 1992).

Contemporary biological systems demonstrate the versatile applications of inorganic NPs across various fields. In biomedicine, iron oxide NPs have shown promise for therapeutic and diagnostic purposes. For example, ferrihydrite NPs exhibiting CAT-like activity, were found to enhance the effectiveness of radiotherapy (Zhang R. et al., 2021), while magnetoferritin NPs have been employed for targeting and visualizing tumor tissues (Fan et al., 2012). Additionally, dietary iron oxide NPs with CAT activity has been shown to mitigate neurodegeneration in a Drosophila-Alzheimer's disease model (Zhang et al., 2016). These findings highlight the potential of iron oxide NPs in addressing aging-related metabolic disorders and neurodegenerative diseases associated with increased ROS production. In agriculture, inorganic NPs have been studied for their effects on plant growth and nutrient uptake. Recent research has indicated their role in enhancing nitrogen fixation, yield, and nutritional quality of soybeans (Cao et al., 2022). Furthermore, foliar application of iron oxide NPs has been observed to stimulate plant growth and act as a defense response against plant viruses (Cai et al., 2020). These findings underscore the potential of inorganic NPs in sustainable agriculture practices. Moreover, inorganic NPs have shown promise in environmental applications, particularly in remediation and pollution control. For instance, green-synthesized magnetite NPs have demonstrated antifungal potential in protecting plants against wilt infection (Ashraf et al., 2022). They have also been effective in mitigating the harmful effects of heavy metal contamination in plants, such as reducing cadmium accumulation in rice biomass (Rizwan et al., 2019; Sarraf et al., 2022; Lu et al., 2023). These applications highlight the diverse potential of inorganic NPs in addressing environmental challenges and contributing to sustainable environmental management.

In summary, the multifaceted applications of inorganic NPs span biomedicine, agriculture and environmental remediation.

Leveraging the functional properties of NPs facilitate a growing number of innovative solutions for a wide range of challenges, from improving human health to enhancing agricultural productivity and addressing environmental pollution.

5 Conclusion

Inorganic 'biocatalysts' were crucial components of prebiotic chemical reactions related to the emergence of life (Bernal, 1951; Williams, 1981; Cairns-Smith, 1985; Williams, 2003), and remain central to many contemporary biological processes. The "metabolism-first" model for the emergence of life posits the development of metabolic networks prior to the emergence of genetic material (Oparin, 1938; Bernal, 1951). This model considers key inorganic processes, such as pyrite formation and serpentinization (Russell and Hall, 1997; Russell et al., 2010; Russell, 2023), which may have played a role in early biochemical reactions due to their surface properties and potential catalytic capabilities (Wächtershäuser, 1992).

Recent perspectives, supported by the discovery of nanocolloidal mineral biocatalyst activity, have shed light on the significance of metal architectures in catalysis, particularly in biological processes (Huang, 2022a). Laboratory studies have demonstrated that inorganic iron-oxide, -sulfide, and -selenide NPs exhibit unique oxidoreductase activity, arising from their metal architecture rather than solely their surface properties. ET and electron hopping within these NPs are influenced by the electronic structure of the metal ions and their coordination with oxygen, sulfur, or other elements, enhancing their oxidoreductase activity. The presence of these inorganic nanocolloids in early Earth environments suggests their involvement in crucial geological and chemical processes, including potential contributions to the first life and the evolution of biological systems.

The essential role of inorganic oxidoreductases in the emergence and evolution of life extends to their influence on the development and adaptation of living organisms over time. These catalysts have been fundamental in shaping the metabolic pathways that form the basis of cellular energy production and utilization using ET. By catalyzing key redox reactions, inorganic oxidoreductases have enabled organisms to efficiently harness and utilize energy from their environments. Furthermore, inorganic oxidoreductases have been involved in biogeochemical cycles that have shaped the availability and cycling of essential elements like carbon, oxygen, phosphorus, sulfur, iron, manganese, and chromium, as well as trace metals such as uranium, in the environment. These cycles play a crucial role in regulating the distribution and cycling of these elements between the atmosphere, lithosphere, hydrosphere, and biosphere.

The discovery of inorganic nano-sized catalysts substantiates the significance of metal architecture in biocatalysts from the onset of the evolution of life on our planet. Furthermore, enhancing our understanding of the contributions of inorganic nanocolloids to the evolution of life may also deepen our understanding of Earth's ecosystems and their interconnectedness. These inorganic nanocolloids and their catalytic activity may have applications in various fields, including biomedicine, agriculture, and

environmental science, owing to their stability and high catalytic efficiency.

Author contributions

X-LH: Conceptualization, Investigation, Validation, Visualization, Writing—original draft, Writing—review and editing. JH: Conceptualization, Investigation, Validation, Visualization, Writing—review and editing. GS: Conceptualization, Investigation, Validation, Visualization, Writing—review and editing. GS: Conceptualization, Investigation, Validation, Visualization, Writing—review and editing.

Funding

The author(s) declare that no financial support was received for the research, authorship, and/or publication of this article.

References

- Abagana, A. Y., Zhao, M., Alshahrani, M. Y., Rehman, K. U., Andleeb, S., Wang, J., et al. (2022). Hydrogen iron oxide from an *Acinetobacter* strain exhibiting intrinsic peroxidase-like activity and its catalytic mechanism and applications. *Biomass Convers. Biorefinery*. doi:10.1007/s13399-022-02370-y
- Adman, E. T., Sieker, L. C., and Jensen, L. H. (1991). Structure of rubredoxin from *Desulfovibrio vulgaris* at 1.5 Å resolution. *J. Mol. Biol.* 217, 337–352. doi:10.1016/0022-2836(91)90547-j
- Agnihotri, S., Mohan, T., Jha, D., Gautam, H. K., and Roy, I. (2020). Dual modality FeS nanoparticles with reactive oxygen species-induced and photothermal toxicity toward pathogenic bacteria. *ACS Omega* 5, 597–602. doi:10.1021/acsomega.9b03177
- Ahmed, A., Abagana, A., Cui, D., and Zhao, M. (2019). *De novo* iron oxide hydroxide, ferrihydrite produced by comamonas testosteroni exhibiting intrinsic peroxidase-like activity and their analytical applications. *Biomed. Res. Int.* 2019, 1–14. doi:10.1155/2019/7127869
- Alexandrov, V., and Rosso, K. M. (2014). Electron transport in pure and substituted iron oxyhydroxides by small-polaron migration. *J. Chem. Phys.* 140, 234701. doi:10.1063/1.4882065
- Alfonso-Prieto, M., Biarnés, X., Vidossich, P., and Rovira, C. (2009). The molecular mechanism of the catalase reaction. *J. Am. Chem. Soc.* 131, 11751–11761. doi:10.1021/ja9018572
- André, R., Natálio, F., Humanes, M., Leppin, J., Heinze, K., Wever, R., et al. (2011). V_2O_5 nanowires with an intrinsic peroxidase-like activity. *Adv. Funct. Mat.* 21, 501–509. doi:10.1002/adfm.201001302
- Apel, K., and Hirt, H. (2004). Reactive oxygen species: metabolism, oxidative stress, and signal transduction. *Ann. Rev. Plant Biol.* 55, 373–399. doi:10.1146/annurev.arplant.55.031903.141701
- Arapova, G. S., Eryomin, A. N., and Metelitza, D. I. (1999). Catalytic peroxidase-like activity of an iron-containing crystallite isolated from ferritin in aqueous solution and reversed micelles of aerosol OT in heptane. *Russ. J. Bioorg. Chem.* 25, 369–376.
- Ashraf, H., Batool, T., Anjum, T., Illyas, A., Li, G., Naseem, S., et al. (2022). Antifungal potential of green synthesized magnetite nanoparticles black coffee–magnetite nanoparticles against wilt infection by ameliorating enzymatic activity and gene expression in *Solanum lycopersicum* L. *Front. Microbiol.* 13, 754292. doi:10.3389/fmicb.2022.754292
- Auffan, M., Achouak, W., Rose, J., Roncato, M. A., Chanéac, C., Waite, D. T., et al. (2008). Relation between the redox state of iron-based nanoparticles and their cytotoxicity toward *Escherichia coli*. *Environ. Sci. Technol.* 42, 6730–6735. doi:10.1021/es800086f
- Baross, J. A., and Hoffman, S. E. (1985). Submarine hydrothermal vents and associated gradient environments as sites for the origin and evolution of life. *Orig. Life Evol. Biosph.* 15, 327–345. doi:10.1007/bf01808177
- Bayr, H. (2005). Reactive oxygen species. *Crit. Care Med.* 33, S498–S501. doi:10.1097/01.ccm.0000186787.64500.12
- Bekker, A., Planavsky, N. J., Krapež, B., Rasmussen, B., Hofmann, A., Slack, J. F., et al. (2013). “Iron formations: their origins and implications for ancient seawater chemistry.” In *Treatise on geochemistry*. Second Edition (Elsevier Inc.), 561–628.
- Berg, I. A., Kockelkorn, D., Ramos-Vera, W. H., Say, R. F., Zarzycki, J., Hügler, M., et al. (2010). Autotrophic carbon fixation in archaea. *Nat. Rev. Microbiol.* 8, 447–460. doi:10.1038/nrmicro2365
- Bernal, J. D. (1951). *The physical basis of life, guthrie lecture*. London: Routledge And Kegan Paul.
- Berstis, L., Beckham, G. T., and Crowley, M. F. (2015). Electronic coupling through natural amino acids. *J. Chem. Phys.* 143, 225102. doi:10.1063/1.4936588
- Bollella, P., Gorton, L., and Antiochia, R. (2018). Direct electron transfer of dehydrogenases for development of 3rd generation biosensors and enzymatic fuel cells. *Sensors* 18, 1319. doi:10.3390/s18051319
- Borda, M. J., Elsetinow, A. R., Schoonen, M. A., and Strongin, D. R. (2001). Pyrite-induced hydrogen peroxide formation as a driving force in the evolution of photosynthetic organisms on an early earth. *Astrobiology* 1, 283–288. doi:10.1089/15311070152757474
- Bostick, C. D., Mukhopadhyay, S., Pecht, I., Sheves, M., Cahen, D., and Lederman, D. (2018). Protein bioelectronics: a review of what we do and do not know. *Rep. Prog. Phys.* 81, 026601. doi:10.1088/1361-6633/aa85f2
- Braterman, P. S., Cairns-Smith, A. G., and Sloper, R. W. (1983). Photo-oxidation of hydrated Fe^{2+} —significance for banded iron formations. *Nature* 303, 163–164. doi:10.1038/303163a0
- Breiter, D. R., Meyer, T. E., Rayment, I., and Holden, H. M. (1991). The molecular structure of the high potential iron-sulfur protein isolated from *Ectothiorhodospira halophila* determined at 2.5-Å resolution. *J. Biol. Chem.* 266, 18660–18667. doi:10.1016/s0021-9258(18)55114-0
- Brown, A. C., Thompson, N. B., and Suess, D. L. M. (2022). Evidence for low-valent electronic configurations in iron–sulfur clusters. *J. Am. Chem. Soc.* 144, 9066–9073. doi:10.1021/jacs.2c01872
- Bruschi, M., and Guerlesquin, F. (1988). Structure, function and evolution of bacterial ferredoxins. *FEMS Microbiol. Lett.* 54, 155–175. doi:10.1111/j.1574-6968.1988.tb02741.x
- Cai, L., Cai, L., Jia, H., Liu, C., Wang, D., and Sun, X. (2020). Foliar exposure of Fe_3O_4 nanoparticles on *Nicotiana benthamiana*: evidence for nanoparticles uptake, plant growth promoter and defense response elicitor against plant virus. *J. Hazard. Mat.* 393, 122415. doi:10.1016/j.jhazmat.2020.122415
- Cairns-Smith, A. G. (1985). *Seven clues to the origin of life, A scientific detective story*. Cambridge, UK: Cambridge University Press.
- Cao, H., Wang, Q., Wang, X., Chen, L., Jiang, J., and Gao, L. (2023). Metastable iron sulfides: a versatile antibacterial candidate with multiple mechanisms against bacterial resistance. *Acc. Mater. Res.* 4, 115–132. doi:10.1021/accountsmr.2c00177
- Cao, X., Yue, L., Wang, C., Luo, X., Zhang, C., Zhao, X., et al. (2022). Foliar application with iron oxide nanomaterials stimulate nitrogen fixation, yield, and nutritional quality of soybean. *ACS Nano* 16, 1170–1181. doi:10.1021/acsnano.1c08977
- Carneiro, L. M., Cushing, S. K., Liu, C., Su, Y., Yang, P., Alivisatos, A. P., et al. (2017). Excitation-wavelength-dependent small polaron trapping of photoexcited carriers in α - Fe_2O_3 . *Nat. Mat.* 16, 819–825. doi:10.1038/nmat4936

Conflict of interest

The authors declare that the research was conducted in the absence of any commercial or financial relationships that could be construed as a potential conflict of interest.

The author(s) declared that they were an editorial board member of Frontiers, at the time of submission. This had no impact on the peer review process and the final decision.

Publisher's note

All claims expressed in this article are solely those of the authors and do not necessarily represent those of their affiliated organizations, or those of the publisher, the editors and the reviewers. Any product that may be evaluated in this article, or claim that may be made by its manufacturer, is not guaranteed or endorsed by the publisher.

- Case, A. J. (2017). On the origin of superoxide dismutase: an evolutionary perspective of superoxide-mediated redox signaling. *Antioxidants* 6, 82. doi:10.3390/antiox6040082
- Cassidy, S. J., Orlandi, F., Manuel, P., and Clarke, S. J. (2019). Single phase charge ordered stoichiometric CaFe_3O_5 with commensurate and incommensurate trimeron ordering. *Nat. Commun.* 10, 5475. doi:10.1038/s41467-019-13450-5
- Castresana, J., Lübben, M., Saraste, M., and Higgins, D. G. (1994). Evolution of cytochrome oxidase, an enzyme older than atmospheric oxygen. *EMBO J.* 13, 2516–2525. doi:10.1002/j.1460-2075.1994.tb06541.x
- Castresana, J., and Saraste, M. (1995). Evolution of energetic metabolism: the respirasome-early hypothesis. *Trends biochem. Sci.* 20, 443–448. doi:10.1016/s0968-0004(00)89098-2
- Castro, L., Tórtora, V., Mansilla, S., and Radi, R. (2019). Aconitases: non-redox iron-sulfur proteins sensitive to reactive species. *Acc. Chem. Res.* 52, 2609–2619. doi:10.1021/acs.accounts.9b00150
- Catling, D. C. (2013). “The Great oxidation event transition,” in *Treatise on geochemistry*. Second Edition (Elsevier Inc.), 177–195.
- Catling, D. C., and Claire, M. W. (2005). How Earth’s atmosphere evolved to an oxic state: a status report. *Earth Planet. Sci. Lett.* 237, 1–20. doi:10.1016/j.epsl.2005.06.013
- Cavalazzi, B., Lemelle, L., Simionovic, A., Cady, S. L., Russell, M. J., Bailo, E., et al. (2021). Cellular remains in a ~3.42-billion-year-old subseafloor hydrothermal environment. *Sci. Adv.* 7, eabf3963. doi:10.1126/sciadv.abf3963
- Chaudhari, K. N., Chaudhari, N. K., and Yu, J. S. (2012). Peroxidase mimic activity of hematite iron oxides ($\alpha\text{-Fe}_2\text{O}_3$) with different nanostructures. *Catal. Sci. Technol.* 2, 119–124. doi:10.1039/c1cy00124h
- Chen, H., Simoska, O., Lim, K., Grattieri, M., Yuan, M., Dong, F., et al. (2020a). Fundamentals, applications, and future directions of bioelectrocatalysis. *Chem. Rev.* 120, 12903–12993. doi:10.1021/acs.chemrev.0c00472
- Chen, J., Ma, Q., Li, M., Wu, W., Huang, L., Liu, L., et al. (2020b). Coenzyme-dependent nanozymes playing dual roles in oxidase and reductase mimics with enhanced electron transport. *Nanoscale* 12, 23578–23585. doi:10.1039/d0nr06605b
- Chen, M., Zhou, X., Xiong, C., Yuan, T., Wang, W., Zhao, Y., et al. (2022). Facet engineering of nanoceria for enzyme-mimetic catalysis. *ACS Appl. Mater Interfaces* 14, 21989–21995. doi:10.1021/acsami.2c04320
- Chen, S., Kang, Z., Zhang, X., Xie, J., Wang, H., Shao, W., et al. (2017). Highly active Fe sites in ultrathin pyrrhotite Fe_2S_8 nanosheets realizing efficient electrocatalytic oxygen evolution. *ACS Cent. Sci.* 3, 1221–1227. doi:10.1021/acscentsci.7b00424
- Chen, T., Zou, H., Wu, X., Liu, C., Situ, B., Zheng, L., et al. (2018). Nanozymatic antioxidant system based on MoS_2 nanosheets. *ACS Appl. Mater Interfaces* 10, 12453–12462. doi:10.1021/acsami.8b01245
- Chen, Z. (2022). Recent development of biomimetic halogenation inspired by vanadium dependent haloperoxidase. *Coord. Chem. Rev.* 457, 214404. doi:10.1016/j.ccr.2021.214404
- Chen, Z., Yin, J. J., Zhou, Y. T., Zhang, Y., Song, L., Song, M., et al. (2012). Dual enzyme-like activities of iron oxide nanoparticles and their implication for diminishing cytotoxicity. *ACS Nano* 6, 4001–4012. doi:10.1021/nm300291r
- Cheng, C.-S., Serizawa, M., Sakata, H., and Hirayama, T. (1998). Electrical conductivity of Co_2O_4 films prepared by chemical vapour deposition. *Mat. Chem. Phys.* 53, 225–230. doi:10.1016/s0254-0584(98)00044-3
- Cheng, X.-L., Jiang, J.-S., Jiang, D.-M., and Zhao, Z.-J. (2014). Synthesis of rhombic dodecahedral Fe_3O_4 nanocrystals with exposed high-energy {110} facets and their peroxidase-like activity and lithium storage properties. *J. Phys. Chem. C* 118, 12588–12598. doi:10.1021/jp412661e
- Chi, Z. L., Zhao, X. Y., Chen, Y. L., Hao, J. L., Yu, G. H., Goodman, B. A., et al. (2021). Intrinsic enzyme-like activity of magnetite particles is enhanced by cultivation with *Trichoderma guizhouense*. *Environ. Microbiol.* 23, 893–907. doi:10.1111/1462-2920.15193
- Chilom, C. G., Zorilă, B., Bacalum, M., Bălășoiu, M., Yaroslavtsev, R., Stolyar, S. V., et al. (2020). Ferrihydrite nanoparticles interaction with model lipid membranes. *Chem. Phys. Lipids*, 226, 104851. doi:10.1016/j.chphylip.2019.104851
- Chong, Y., Liu, Q., and Ge, C. (2021). Advances in oxidase-mimicking nanozymes: classification, activity regulation and biomedical applications. *Nano Today* 37, 101076. doi:10.1016/j.nantod.2021.101076
- Claudio, C., Di Iorio, E., Liu, Q., Jiang, Z., and Barrón, V. (2017). Iron oxide nanoparticles in soils: environmental and agronomic importance. *J. Nanosci. Nanotechnol.* 17, 4449–4460. doi:10.1166/jnn.2017.14197
- Cornell, R. M., and Schwertmann, U. (2003). *The iron oxides: structure, properties, reactions, occurrence and uses*. Wiley-VCH Verlag GmbH and Co. KGaA.
- Cui, Z., Li, Y., Zhang, H., Qin, P., Hu, X., Wang, J., et al. (2022). Lighting up agricultural sustainability in the new era through nanozymology: an overview of classifications and their agricultural applications. *J. Agric. Food Chem.* 70, 13445–13463. doi:10.1021/acs.jafc.2c04882
- Dai, Z., Liu, S., Bao, J., and Ju, H. (2009). Nanostructured FeS as a mimic peroxidase for biocatalysis and biosensing. *Chemistry* 15, 4321–4326. doi:10.1002/chem.200802158
- De Aldecoa, A. L., Roldán, F. V., and Menor-Salván, C. (2013). Natural pyrrhotite as a catalyst in prebiotic chemical evolution. *Life* 3, 502–517. doi:10.3390/life3030502
- De Duve, C. (1991). *Blueprint for a cell: the nature and origin of life*. Burlington, North Carolina: Neil Patterson Publishers.
- Deisseroth, A., and Dounce, A. L. (1970). Catalase: physical and chemical properties, mechanism of catalysis, and physiological role. *Physiol. Rev.* 50, 319–375. doi:10.1152/physrev.1970.50.3.319
- De Oliveira, F. K., Santos, L. O., and Buffon, J. G. (2021). Mechanism of action, sources, and application of peroxidases. *Food Res. Int.* 143, 110266. doi:10.1016/j.foodres.2021.110266
- Devaraj, S., and Munichandraiah, N. (2008). Effect of crystallographic structure of MnO_2 on its electrochemical capacitance properties. *J. Phys. Chem. C* 112, 4406–4417. doi:10.1021/jp7108785
- Devey, A. J., Grau-Crespo, R., and De Leeuw, N. H. (2009). Electronic and magnetic structure of Fe_3S_4 : GGA+U investigation. *Phys. Rev. B* 79, 195126. doi:10.1103/physrevb.79.195126
- Dhall, A., Burns, A., Dowding, J., Das, S., Seal, S., and Self, W. (2017). Characterizing the phosphatase mimetic activity of cerium oxide nanoparticles and distinguishing its active site from that for catalase mimetic activity using anionic inhibitors. *Environ. Sci. Nano* 4, 1742–1749. doi:10.1039/c7en00394c
- Ding, C., Yan, Y., Xiang, D., Zhang, C., and Xian, Y. (2016). Magnetic Fe_3S_4 nanoparticles with peroxidase-like activity, and their use in a photometric enzymatic glucose assay. *Microchim. Acta* 183, 625–631. doi:10.1007/s00604-015-1690-6
- Ding, W., Liu, H., Zhao, W., Wang, J., Zhang, L., Yao, Y., et al. (2020a). A hybrid of FeS_2 nanoparticles encapsulated by two-dimensional carbon sheets as excellent nanozymes for colorimetric glucose detection. *ACS Appl. Bio Mat.* 3, 5905–5912. doi:10.1021/acsabm.0c00605
- Ding, Y., Ren, G., Wang, G., Lu, M., Liu, J., Li, K., et al. (2020b). V_2O_5 nanobelts mimick tandem enzymes to achieve nonenzymatic online monitoring of glucose in living rat brain. *Anal. Chem.* 92, 4583–4591. doi:10.1021/acs.analchem.9b05872
- Dixon, D. A., and Lipscomb, W. N. (1976). Electronic structure and bonding of the amino acids containing first row atoms. *J. Biol. Chem.* 251, 5992–6000. doi:10.1016/s0021-9258(17)33049-1
- Dong, H., Du, W., Dong, J., Che, R., Kong, F., Cheng, W., et al. (2022). Depletable peroxidase-like activity of Fe_3O_4 nanozymes accompanied with separate migration of electrons and iron ions. *Nat. Commun.* 13, 5365. doi:10.1038/s41467-022-33098-y
- Drennan, C. L., and Peters, J. W. (2003). Surprising cofactors in metalloenzymes. *Curr. Opin. Struct. Biol.* 13, 220–226. doi:10.1016/s0959-440x(03)00038-1
- Dröge, W. (2002). Free radicals in the physiological control of cell function. *Physiol. Rev.* 82, 47–95. doi:10.1152/physrev.00018.2001
- Dupuy, J., Volbeda, A., Carpentier, P., Darnault, C., Moulis, J. M., and Fontecilla-Camps, J. C. (2006). Crystal structure of human iron regulatory protein 1 as cytosolic aconitase. *Structure* 14, 129–139. doi:10.1016/j.str.2005.09.009
- Dutta, A. K., Das, S., Samanta, S., Samanta, P. K., Adhikary, B., and Biswas, P. (2013). CuS nanoparticles as a mimic peroxidase for colorimetric estimation of human blood glucose level. *Talanta* 107, 361–367. doi:10.1016/j.talanta.2013.01.032
- Dutta, A. K., Maji, S. K., Mondal, A., Karmakar, B., Biswas, P., and Adhikary, B. (2012a). Iron selenide thin film: peroxidase-like behavior, glucose detection and amperometric sensing of hydrogen peroxide. *Sens. Actuators B Chem.* 173, 724–731. doi:10.1016/j.snb.2012.07.070
- Dutta, A. K., Maji, S. K., Srivastava, D. N., Mondal, A., Biswas, P., Paul, P., et al. (2012b). Synthesis of FeS and FeSe nanoparticles from a single source precursor: a study of their photocatalytic activity, peroxidase-like behavior, and electrochemical sensing of H_2O_2 . *ACS Appl. Mater Interfaces* 4, 1919–1927. doi:10.1021/am300408r
- Dwyer, D. S. (2006). Nearest-neighbor effects and structural preferences in dipeptides are a function of the electronic properties of amino acid side-chains. *Proteins* 63, 939–948. doi:10.1002/prot.20906
- Eck, R. V., and Dayhoff, M. O. (1966). Evolution of the structure of ferredoxin based on living relics of primitive amino Acid sequences. *Science* 152, 363–366. doi:10.1126/science.152.3720.363
- Eddowes, M. J., and Hill, H. a.O. (1977). Novel method for the investigation of the electrochemistry of metalloproteins: cytochrome c. *J. Chem. Soc. Chem. Commun.*, 771b–772b. doi:10.1039/c3977000771b
- Erlebach, A., Kurland, H.-D., Grabow, J., Müller, F. A., and Sierka, M. (2015). Structure evolution of nanoparticulate Fe_2O_3 . *Nanoscale* 7, 2960–2969. doi:10.1039/c4nr06989g
- Esch, F., Fabris, S., Zhou, L., Montini, T., Africh, C., Fornasiero, P., et al. (2005). Electron localization determines defect formation on ceria substrates. *Science* 309, 752–755. doi:10.1126/science.1111568
- Falkowski, P. G., Fenchel, T., and Delong, E. F. (2008). The microbial engines that drive earth’s biogeochemical cycles. *Science* 320, 1034–1039. doi:10.1126/science.1153213
- Fan, K., Cao, C., Pan, Y., Lu, D., Yang, D., Feng, J., et al. (2012). Magnetoferritin nanoparticles for targeting and visualizing tumour tissues. *Nat. Nanotechnol.* 7, 765–464. doi:10.1038/nnano.2012.204

- Fan, K., Wang, H., Xi, J., Liu, Q., Meng, X., Duan, D., et al. (2017). Optimization of Fe_3O_4 nanzyme activity via single amino acid modification mimicking an enzyme active site. *Chem. Commun.* 53, 424–427. doi:10.1039/c6cc08542c
- Faroog, M. U., Muhammad, Z., Khalid, S., Fatima, K., and Zou, B. (2019). Magnetic coupling in 3D-hierarchical MnO_2 microsphere. *J. Mat. Sci. Mat. Electron.* 30, 2802–2808. doi:10.1007/s10854-018-0556-1
- Ferapontova, E. E., Ruzgas, T., and Gorton, L. (2003). Direct electron transfer of heme- and molybdopterin cofactor-containing chicken liver sulfite oxidase on alkane-thiol-modified gold electrodes. *Anal. Chem.* 75, 4841–4850. doi:10.1021/ac0341923
- Ferus, M., Pietrucci, F., Saitta, A. M., Knižek, A., Kubelík, P., Ivanek, O., et al. (2017). Formation of nucleobases in a Miller–Urey reducing atmosphere. *Proc. Natl. Acad. Sci. U. S. A.* 114, 4306–4311. doi:10.1073/pnas.1700010114
- Findlay, A. J., Estes, E. R., Gartman, A., Yücel, M., Kamyshny, A., and Luther, G. W. (2019). Iron and sulfide nanoparticle formation and transport in nascent hydrothermal vent plumes. *Nat. Commun.* 10, 1597. doi:10.1038/s41467-019-09580-5
- Frenkel-Pinter, M., Bouza, M., Fernández, F. M., Leman, L. J., Williams, L. D., Hud, N. V., et al. (2022). Thioesters provide a plausible prebiotic path to proto-peptides. *Nat. Commun.* 13, 2569. doi:10.1038/s41467-022-30191-0
- Fridovich, I. (1995). Superoxide radical and superoxide dismutases. *Annu. Rev. Biochem.* 64, 97–112. doi:10.1146/annurev.bi.64.070195.000525
- Gao, L. (2022). “Enzyme-like property (nanzyme) of iron oxide nanoparticles,” in *Iron oxide nanoparticles*. Editor X. L. Huang (London UK: Intechopen).
- Gao, L., Fan, K., and Yan, X. (2017). Iron oxide nanzyme: a multifunctional enzyme mimetic for biomedical applications. *Theranostics* 7, 3207–3227. doi:10.7150/thno.19738
- Gao, L., and Yan, X. (2019). Nanozymes: biomedical applications of enzymatic Fe_3O_4 nanoparticles from *in vitro* to *in vivo*. *Adv. Exp. Med. Biol.* 1174, 291–312. doi:10.1007/978-981-13-9791-2_9
- Gao, L., Zhuang, J., Nie, L., Zhang, J., Zhang, Y., Gu, N., et al. (2007). Intrinsic peroxidase-like activity of ferromagnetic nanoparticles. *Nat. Nanotechnol.* 2, 577–583. doi:10.1038/nnano.2007.260
- Geng, R., Chang, R., Zou, Q., Shen, G., Jiao, T., and Yan, X. (2021). Biomimetic nanozymes based on coassembly of amino acid and hemin for catalytic oxidation and sensing of biomolecules. *Small* 17, 2008114. doi:10.1002/smll.202008114
- Ghosh, S., Roy, P., Karmodak, N., Jemmis, E. D., and Muges, G. (2018). Nanoisozymes: crystal-facet-dependent enzyme-mimetic activity of V_2O_5 nanomaterials. *Angew. Chem. Int. Ed.* 57, 4510–4515. doi:10.1002/anie.201800681
- Giese, B. (2018). “Electron hopping in biomolecules,” in *Encyclopedia of biophysics*. Editors G. Roberts, and A. Watts (Berlin, Heidelberg: Springer Berlin Heidelberg), 1–3.
- Gomes, R., Levison, H. F., Tsiganis, K., and Morbidelli, A. (2005). Origin of the cataclysmic Late Heavy Bombardment period of the terrestrial planets. *Nature* 435, 466–469. doi:10.1038/nature03676
- Gonet, T., and Maher, B. A. (2019). Airborne, vehicle-derived Fe-bearing nanoparticles in the urban environment: a review. *Environ. Sci. Technol.* 53, 9970–9991. doi:10.1021/acs.est.9b01505
- Gorton, L., Lindgren, A., Larsson, T., Munteanu, F. D., Ruzgas, T., and Gazaryan, I. (1999). Direct electron transfer between heme-containing enzymes and electrodes as basis for third generation biosensors. *Anal. Chim. Acta* 400, 91–108. doi:10.1016/s0003-2670(99)00610-8
- Goswami, P., He, K., Li, J., Pan, Y., Roberts, A. P., and Lin, W. (2022). Magnetotactic bacteria and magnetofossils: ecology, evolution and environmental implications. *NPJ Biofilms Microbiomes* 8, 43. doi:10.1038/s41522-022-00304-0
- Grau-Crespo, R., Al-Baitai, A. Y., Saadoune, I., and De Leeuw, N. H. (2010). Vacancy ordering and electronic structure of $\gamma\text{-Fe}_2\text{O}_3$ (maghemite): a theoretical investigation. *J. Phys. Condens. Matter* 22, 255401. doi:10.1088/0953-8984/22/25/255401
- Gray, H. B., and Winkler, J. R. (2015). Hole hopping through tyrosine/tryptophan chains protects proteins from oxidative damage. *Proc. Natl. Acad. Sci. U. S. A.* 112, 10920–10925. doi:10.1073/pnas.1512704112
- Gray, H. B., and Winkler, J. R. (2021). Functional and protective hole hopping in metalloenzymes. *Chem. Sci.* 12, 13988–14003. doi:10.1039/d1sc04286f
- Grishin, N. V. (2001). Fold change in evolution of protein structures. *J. Struct. Biol.* 134, 167–185. doi:10.1006/jbsb.2001.4335
- Gu, X., Heaney, P. J., Reis, F. D. a. A., and Brantley, S. L. (2020a). Deep abiotic weathering of pyrite. *Science* 370, eabb8092. doi:10.1126/science.abb8092
- Gu, Y., Huang, Y., Qiu, Z., Xu, Z., Li, D., Chen, L., et al. (2020b). Vitamin B(2) functionalized iron oxide nanozymes for mouth ulcer healing. *Sci. China Life Sci.* 63, 68–79. doi:10.1007/s11427-019-9590-6
- Guo, H., and Barnard, A. S. (2013). Naturally occurring iron oxide nanoparticles: morphology, surface chemistry and environmental stability. *J. Mater. Chem. A* 1, 27–42. doi:10.1039/c2ta00523a
- Guo, S., and Guo, L. (2019). Unraveling the multi-enzyme-like activities of iron oxide nanzyme via a first-principles microkinetic study. *J. Phys. Chem. C* 123, 30318–30334. doi:10.1021/acs.jpcc.9b07802
- Guo, Z., Sun, F., Han, B., Lin, K., Zhou, L., and Yuan, W. (2017). Iron vacancy in tetragonal $\text{FeI}-x\text{S}$ crystals and its effect on the structure and superconductivity. *Phys. Chem. Chem. Phys.* 19, 9000–9006. doi:10.1039/c7cp00068e
- Gurbiel, R. J., Doan, P. E., Gassner, G. T., Macke, T. J., Case, D. A., Ohnishi, T., et al. (1996). Active site structure of Rieske-type proteins: electron nuclear double resonance studies of isotopically labeled phthalate dioxygenase from *Pseudomonas cepacia* and Rieske protein from Rhodobacter capsulatus and molecular modeling studies of a Rieske center. *Biochemistry* 35, 7834–7845. doi:10.1021/bi960380u
- Halevy, I., Alešker, M., Schuster, E. M., Popovitz-Biro, R., and Feldman, Y. (2017). A key role for green rust in the Precambrian oceans and the genesis of iron formations. *Nat. Geosci.* 10, 135–139. doi:10.1038/ngeo2878
- Hall, A., Nelson, K., Poole, L. B., and Karplus, P. A. (2011). Structure-based insights into the catalytic power and conformational dexterity of peroxiredoxins. *Antioxid. Redox Signal.* 15, 795–815. doi:10.1089/ars.2010.3624
- Halliwell, B. (2006). Reactive species and antioxidants. Redox biology is a fundamental theme of aerobic life. *Plant Physiol.* 141, 312–322. doi:10.1104/pp.106.077073
- Halpern, J., and Orgel, L. E. (1960). The theory of electron transfer between metal ions in bridged systems. *Discuss. Faraday Soc.* 29, 32–41. doi:10.1039/df9602900032
- Han, J., Gong, H., Ren, X., and Yan, X. (2021). Supramolecular nanozymes based on peptide self-assembly for biomimetic catalysis. *Nano Today* 41, 101295. doi:10.1016/j.nantod.2021.101295
- Han, J., Zou, Q., Su, W., and Yan, X. (2020). Minimal metallo-nanozymes constructed through amino acid coordinated self-assembly for hydrolase-like catalysis. *Chem. Eng. J.* 394, 124987. doi:10.1016/j.cej.2020.124987
- Hawkins, J. R., Wadham, J. L., Tranter, M., Raiswell, R., Benning, L. G., Statham, P. J., et al. (2014). Ice sheets as a significant source of highly reactive nanoparticulate iron to the oceans. *Nat. Commun.* 5, 3929. doi:10.1038/ncomms4929
- He, H., Wu, X., Xian, H., Zhu, J., Yang, Y., Lv, Y., et al. (2021). An abiotic source of Archean hydrogen peroxide and oxygen that pre-dates oxygenic photosynthesis. *Nat. Commun.* 12, 6611. doi:10.1038/s41467-021-26916-2
- Herschy, B., Whicher, A., Camprubi, E., Watson, C., Dartnell, L., Ward, J., et al. (2014). An origin-of-life reactor to simulate alkaline hydrothermal vents. *J. Mol. Evol.* 79, 213–227. doi:10.1007/s00239-014-9658-4
- Hille, R., Hall, J., and Basu, P. (2014). The mononuclear molybdenum enzymes. *Chem. Rev.* 114, 3963–4038. doi:10.1021/cr400443z
- Hofmann, A., and Bolhar, R. (2007). Carbonaceous cherts in the barberton greenstone belt and their significance for the study of early life in the archean record. *Astrobiology* 7, 355–388. doi:10.1089/ast.2005.0288
- Holden, H. M., Jacobson, B. L., Hurley, J. K., Tollin, G., Oh, B. H., Skjeldal, L., et al. (1994). Structure-function studies of [2Fe-2S] ferredoxins. *J. Bioenerg. Biomembr.* 26, 67–88. doi:10.1007/bf00763220
- Holland, H. D. (2007). “The geologic history of seawater,” in *Treatise on geochemistry* (Elsevier Inc.), 1–46.
- Holm, R. H., Kennepohl, P., and Solomon, E. I. (1996). Structural and functional aspects of metal sites in biology. *Chem. Rev.* 96, 2239–2314. doi:10.1021/cr9500390
- Hong, C., Meng, X., He, J., Fan, K., and Yan, X. (2022). Nanozyme: a promising tool from clinical diagnosis and environmental monitoring to wastewater treatment. *Particuology* 71, 90–107. doi:10.1016/j.partic.2022.02.001
- Hong, K. H., Arevalo-Lopez, A. M., Cumby, J., Ritter, C., and Attfield, J. P. (2018). Long range electronic phase separation in CaFe_3O_5 . *Nat. Commun.* 9, 2975. doi:10.1038/s41467-018-05363-6
- Hopfield, J. J. (1974). Electron transfer between biological molecules by thermally activated tunneling. *Proc. Natl. Acad. Sci. U. S. A.* 71, 3640–3644. doi:10.1073/pnas.71.9.3640
- Hsu, F.-C., Luo, J.-Y., Yeh, K.-W., Chen, T.-K., Huang, T.-W., Wu, P. M., et al. (2008). Superconductivity in the PbO-type structure $\alpha\text{-FeSe}$. *Proc. Natl. Acad. Sci. U. S. A.* 105, 14262–14264. doi:10.1073/pnas.0807325105
- Hu, L., Song, T., Ma, Q., Chen, C., Pan, W., Xie, C., et al. (2010). Bacterial magnetic nanoparticles as peroxidase mimetics and application in immunoassay. *AIP Conf. Proc.* 1311, 369–374. doi:10.1063/1.3530039
- Huang, C., Liu, Z., Chen, M., Du, L., Liu, C., Wang, S., et al. (2021). Tumor-derived biomimetic nanozyme with immune evasion ability for synergistically enhanced low dose radiotherapy. *J. Nanobiotechnology* 19, 457. doi:10.1186/s12951-021-01182-y
- Huang, X., Ramadugu, S. K., and Mason, S. E. (2016a). Surface-specific DFT + U approach applied to $\alpha\text{-Fe}_2\text{O}_3(0001)$. *J. Phys. Chem. C* 120, 4919–4930. doi:10.1021/acs.jpcc.5b12144
- Huang, X. L. (2018). Hydrolysis of phosphate esters catalyzed by inorganic iron oxide nanoparticles acting as biocatalysts. *Astrobiology* 18, 294–310. doi:10.1089/ast.2016.1628
- Huang, X. L. (2019). “Iron oxide nanoparticles: an inorganic phosphatase,” in *Nanocatalysts*. Editors I. Sinha, and M. Shukla (London: Intechopen), 97–124.
- Huang, X.-L. (2022a). What are inorganic nanozymes? Artificial or inorganic enzymes. *New J. Chem.* 46, 15273–15291. doi:10.1039/d2nj02088b

- Huang, X. L. (2022b). "Introduction chapter, incredible spicy iron oxide nanoparticles," in *Iron oxide nanoparticles*. Editor X.-L. Huang (London: intechopen.com), 1–20.
- Huang, X. L., and Zhang, J. Z. (2007). "Sediment-water exchange of dissolved organic phosphorus in Florida bay," in *CIMAS seventh year annual report (NOAA cooperative agreement NA17RJ1226)*. Editors P. O. Joseph, and M. Prospero (Miami, FL, USA: University of Miami).
- Huang, X. L., and Zhang, J. Z. (2012). Hydrolysis of glucose-6-phosphate in aged, acid-forced hydrolysed nanomolar inorganic iron solutions - an inorganic biocatalyst? *RSC Adv.* 2, 199–208. doi:10.1039/c1ra00353d
- Huang, Y., Liu, Z., Liu, C., Ju, E., Zhang, Y., Ren, J., et al. (2016b). Self-Assembly of multi-nanozymes to mimic an intracellular antioxidant defense system. *Angew. Chem. Int. Ed.* 55, 6646–6650. doi:10.1002/anie.201600868
- Huang, Y., Ren, J., and Qu, X. (2019). Nanozymes: classification, catalytic mechanisms, activity regulation, and applications. *Chem. Rev.* 119, 4357–4412. doi:10.1021/acs.chemrev.8b00672
- Husek, J., Cirri, A., Biswas, S., and Baker, L. R. (2017). Surface electron dynamics in hematite (α -Fe₂O₃): correlation between ultrafast surface electron trapping and small polaron formation. *Chem. Sci.* 8, 8170–8178. doi:10.1039/c7sc02826a
- Ibrahim, E. M. M., Abdel-Rahman, L. H., Abu-Dief, A. M., Elshafaie, A., Hamdan, S. K., and Ahmed, A. M. (2018). Electric, thermoelectric and magnetic characterization of γ -Fe₂O₃ and Co₃O₄ nanoparticles synthesized by facile thermal decomposition of metal-Schiff base complexes. *Mat. Res. Bull.* 99, 103–108. doi:10.1016/j.materresbull.2017.11.002
- Imlay, J. A. (2006). Iron-sulphur clusters and the problem with oxygen. *Mol. Microbiol.* 59, 1073–1082. doi:10.1111/j.1365-2958.2006.05028.x
- Inupakutika, M. A., Sengupta, S., Devireddy, A. R., Azad, R. K., and Mittler, R. (2016). The evolution of reactive oxygen species metabolism. *J. Exp. Bot.* 67, 5933–5943. doi:10.1093/jxb/erw382
- Iordanova, N., Dupuis, M., and Rosso, K. M. (2005). Charge transport in metal oxides: a theoretical study of hematite alpha-Fe₂O₃. *J. Chem. Phys.* 122, 144305. doi:10.1063/1.1869492
- Ito, T., Takagi, H., Ishibashi, S., Ido, T., and Uchida, S. (1991). Normal-state conductivity between CuO₂ planes in copper oxide superconductors. *Nature* 350, 596–598. doi:10.1038/350596a0
- Jamilpanah, P., Pahlavanzadeh, H., and Kheradmand, A. (2017). Thermal conductivity, viscosity, and electrical conductivity of iron oxide with a cloud fractal structure. *Heat. Mass Transf.* 53, 1343–1354. doi:10.1007/s00231-016-1891-5
- Jancura, D., Stanicova, J., Palmer, G., and Fabian, M. (2014). How hydrogen peroxide is metabolized by oxidized cytochrome c oxidase. *Biochemistry* 53, 3564–3575. doi:10.1017/bi.2010.78b
- Jenkins, J. M., Brune, W. H., and Miller, D. O. (2021). Electrical discharges produce prodigious amounts of hydroxyl and hydroperoxyl radicals. *J. Geophys. Res. Atmos.* 126, e2021JD04557. doi:10.1029/2021jd034557
- Jian, W., Wang, S.-P., Zhang, H.-X., and Bai, F.-Q. (2019). Disentangling the role of oxygen vacancies on the surface of Fe₃O₄ and γ -Fe₂O₃. *Inorg. Chem. Front.* 6, 2660–2666. doi:10.1039/c9qi00351g
- Jiang, Y., Xia, T., Shen, L., Ma, J., Ma, H., Sun, T., et al. (2021). Facet-Dependent Cu₂O electrocatalysis for wearable enzyme-free smart sensing. *ACS Catal.* 11, 2949–2955. doi:10.1021/acscatal.0c04797
- Johnson, A. P., Cleaves, H. J., Dworkin, J. P., Glavin, D. P., Lazcano, A., and Bada, J. L. (2008). The miller volcanic spark discharge experiment. *Science* 322, 404. doi:10.1126/science.1161527
- Jolivet, J. P. (2019). *Metal oxide nanostructures chemistry: synthesis from aqueous solutions*. New York: Oxford University Press.
- Jolivet, J.-P., and Tronc, E. (1988). Interfacial electron transfer in colloidal spinel iron oxide. Conversion of Fe₃O₄- γ Fe₂O₃ in aqueous medium. *J. Colloid Interface Sci.* 125, 688–701. doi:10.1016/0021-9797(88)90036-7
- Jolivet, J. P., Tronc, E., and Chanéac, C. (2006). Iron oxides: from molecular clusters to solid. A nice example of chemical versatility. *CR Geosci.* 338, 488–497. doi:10.1002/chin.200605225
- Kantar, C., Oral, O., and Oz, N. A. (2019). Ligand enhanced pharmaceutical wastewater treatment with Fenton process using pyrite as the catalyst: column experiments. *Chemosphere* 237, 124440. doi:10.1016/j.chemosphere.2019.124440
- Kappler, A., Bryce, C., Mansor, M., Lueder, U., Byrne, J. M., and Swanner, E. D. (2021). An evolving view on biogeochemical cycling of iron. *Nat. Rev. Microbiol.* 19, 360–374. doi:10.1038/s41579-020-00502-7
- Kappler, U., and Enemark, J. H. (2015). Sulfite-oxidizing enzymes. *J. Biol. Inorg. Chem.* 20, 253–264. doi:10.1007/s00775-014-1197-3
- Kasting, J. F. (1993). Earth's early atmosphere. *Science* 259, 920–926. doi:10.1126/science.11536547
- Kasting, J. F., Pollack, J. B., and Crisp, D. (1984). Effects of high CO₂ levels on surface temperature and atmospheric oxidation state of the early Earth. *J. Atmos. Chem.* 1, 403–428. doi:10.1007/bf00053803
- Katz, J. E., Zhang, X., Attenkofer, K., Chapman, K. W., Frandsen, C., Zarzycki, P., et al. (2012). Electron small polarons and their mobility in iron (oxyhydr)oxide nanoparticles. *Science* 337, 1200–1203. doi:10.1126/science.1223598
- Katzen, F., and Beckwith, J. (2000). Transmembrane electron transfer by the membrane protein DsbD occurs via a disulfide bond cascade. *Cell* 103, 769–779. doi:10.1016/s0092-8674(00)00180-x
- Kerisit, S., and Rosso, K. M. (2006). Computer simulation of electron transfer at hematite surfaces. *Geochim. Cosmochim. Acta* 70, 1888–1903. doi:10.1016/j.gca.2005.12.021
- Kim, J. D., Senn, S., Harel, A., Jelen, B. I., and Falkowski, P. G. (2013). Discovering the electronic circuit diagram of life: structural relationships among transition metal binding sites in oxidoreductases. *Philos. Trans. R. Soc. Lond., B, Biol. Sci.* 368, 20120257. doi:10.1098/rstb.2012.0257
- Kim, S., and Maier, J. (2002). On the conductivity mechanism of nanocrystalline ceria. *J. Electrochem. Soc.* 149, J73. doi:10.1149/1.1507597
- Knauth, L. P., and Lowe, D. R. (2003). High Archean climatic temperature inferred from oxygen isotope geochemistry of cherts in the 3.5 Ga Swaziland Supergroup, South Africa. *Geol. Soc. Am. Bull.* 115, 566–580. doi:10.1130/0016-7606(2003)115<0566:hactif>2.0.co;2
- Konishi, H., Xu, H., and Guo, H. (2012). "Nanostructures of natural iron oxide nanoparticles," in *Nature's nanostructures*. Editors A. S. Barnard and H. Guo (New York: Jenny Stanford Publishing), 75–113.
- Krake, F., Vassilev, I., and Krömer, J. O. (2015). Microbial electron transport and energy conservation - the foundation for optimizing bioelectrochemical systems. *Front. Microbiol.* 6, 575. doi:10.3389/fmicb.2015.00575
- Krupp, R., Chan, C., and Missiakas, D. (2001). DsbD-catalyzed transport of electrons across the membrane of *Escherichia coli*. *J. Biol. Chem.* 276, 3696–3701. doi:10.1074/jbc.m009500200
- Kuhn, S. J., Kidder, M. K., Parker, D. S., Dela Cruz, C., McGuire, M. A., Chance, W. M., et al. (2017). Structure and property correlations in FeS. *Phys. C Supercond.* 534, 29–36. doi:10.1016/j.physc.2016.12.006
- Lai, X., Zhang, H., Wang, Y., Wang, X., Zhang, X., Lin, J., et al. (2015). Observation of superconductivity in tetragonal FeS. *J. Am. Chem. Soc.* 137, 10148–10151. doi:10.1021/jacs.5b06687
- Leblanc, C., Vilte, H., Fournier, J. B., Delage, L., Potin, P., Rebuffet, E., et al. (2015). Vanadium haloperoxidases: from the discovery 30 years ago to X-ray crystallographic and V K-edge absorption spectroscopic studies. *Coord. Chem. Rev.* 301–302, 134–146. doi:10.1016/j.ccr.2015.02.013
- Lee, C. C., Hu, Y., and Ribbe, M. W. (2010). Vanadium nitrogenase reduces CO. *Science* 329, 642. doi:10.1126/science.1191455
- Lee, J. K., Walker, K. L., Han, H. S., Kang, J., Prinz, F. B., Waymouth, R. M., et al. (2019). Spontaneous generation of hydrogen peroxide from aqueous microdroplets. *Proc. Natl. Acad. Sci. U. S. A.* 116, 19294–19298. doi:10.1073/pnas.1911883116
- Léger, C., and Bertrand, P. (2008). Direct electrochemistry of redox enzymes as a tool for mechanistic studies. *Chem. Rev.* 108, 2379–2438. doi:10.1021/cr0680742
- Lenton, T. M. (2003). "The coupled evolution of life and atmospheric oxygen," in *Evolution on planet Earth: the impact of the physical environment* (Elsevier Ltd), 35–53.
- Leskovac, V., Trivić, S., Wohlfahrt, G., Kandrač, J., and Peričin, D. (2005). Glucose oxidase from *Aspergillus Niger*: the mechanism of action with molecular oxygen, quinones, and one-electron acceptors. *Int. J. Biochem. Cell Biol.* 37, 731–750. doi:10.1016/j.biocel.2004.10.014
- Li, G., Zhang, B., Yu, F., Novakova, A. A., Krivenkov, M. S., Kiseleva, T. Y., et al. (2014). High-purity Fe₃S₄ greigite microcrystals for magnetic and electrochemical performance. *Chem. Mat.* 26, 5821–5829. doi:10.1021/cm501493m
- Li, K., Chen, C., Chen, C., Wang, Y., Wei, Z., Pan, W., et al. (2015). Magnetosomes extracted from *Magnetospirillum magneticum* strain AMB-1 showed enhanced peroxidase-like activity under visible-light irradiation. *Enzyme Microb. Technol.* 72, 72–78. doi:10.1016/j.enzmictec.2015.02.009
- Li, Q., Kartikowati, C. W., Horie, S., Ogi, T., Iwaki, T., and Okuyama, K. (2017). Correlation between particle size/domain structure and magnetic properties of highly crystalline Fe₃O₄ nanoparticles. *Sci. Rep.* 7, 9894. doi:10.1038/s41598-017-09897-5
- Liu, W., Wang, J., Zhu, J., and Zheng, Y.-Q. (2018). Co₃O₄ nanocrystals as an efficient catalase mimic for the colorimetric detection of glutathione. *J. Mater. Chem. B* 6, 6858–6864. doi:10.1039/c8tb01948f
- Liang, M., and Yan, X. (2019). Nanozymes: from new concepts, mechanisms, and standards to applications. *Acc. Chem. Res.* 52, 2190–2200. doi:10.1021/acs.accounts.9b00140
- Liang, M. C., Hartman, H., Kopp, R. E., Kirschvink, J. L., and Yung, Y. L. (2006). Production of hydrogen peroxide in the atmosphere of a Snowball Earth and the origin of oxygenic photosynthesis. *Proc. Natl. Acad. Sci. U. S. A.* 103, 18896–18899. doi:10.1073/pnas.0608839103
- Liu, F., Geng, J., Gumpfer, R. H., Barman, A., Davis, I., Ozarowski, A., et al. (2015). An iron reservoir to the catalytic metal: the rubredoxin iron in an extradiol dioxygenase. *J. Biol. Chem.* 290, 15621–15634. doi:10.1074/jbc.m115.650259

- Liu, J., Chakraborty, S., Hosseinzadeh, P., Yu, Y., Tian, S., Petrik, I., et al. (2014). Metalloproteins containing cytochrome, iron-sulfur, or copper redox centers. *Chem. Rev.* 114, 4366–4469. doi:10.1021/cr400479b
- Liu, K., Ma, X., Xu, S., Li, Y., and Zhao, M. (2023). Tunable sliding ferroelectricity and magnetoelectric coupling in two-dimensional multiferroic MnSe materials. *NPJ Comput. Mater.* 9, 16. doi:10.1038/s41524-023-00972-2
- Liu, S., Lu, F., Xing, R., and Zhu, J. J. (2011). Structural effects of Fe_3O_4 nanocrystals on peroxidase-like activity. *Chem. Eur. J.* 17, 620–625. doi:10.1002/chem.201001789
- Liu, T., Xiao, B., Xiang, F., Tan, J., Chen, Z., Zhang, X., et al. (2020a). Ultrasmall copper-based nanoparticles for reactive oxygen species scavenging and alleviation of inflammation related diseases. *Nat. Commun.* 11, 2788. doi:10.1038/s41467-020-16544-7
- Liu, W., Tian, J., Mao, C., Wang, Z., Liu, J., Dahlgren, R. A., et al. (2020b). Sulfur vacancy promoted peroxidase-like activity of magnetic greigite (Fe_3S_4) for colorimetric detection of serum glucose. *Anal. Chim. Acta* 1127, 246–255. doi:10.1016/j.aca.2020.06.056
- Liu, Y., Xiao, Z., Chen, F., Yue, L., Zou, H., Lyu, J., et al. (2021). Metallic oxide nanomaterials act as antioxidant nanozymes in higher plants: trends, meta-analysis, and prospect. *Sci. Total Environ.* 780, 146578. doi:10.1016/j.scitotenv.2021.146578
- Liu, Y., Yuan, R., Chai, Y., Tang, D., Dai, J., and Zhong, X. (2006). Direct electrochemistry of horseradish peroxidase immobilized on gold colloid/cysteine/nafion-modified platinum disk electrode. *Sens. Actuators B Chem.* 115, 109–115. doi:10.1016/j.snb.2005.08.048
- Lopez-Cantu, D. O., González-González, R. B., Sharma, A., Bilal, M., Parra-Saldívar, R., and Iqbal, H. M. N. (2022). Bioactive material-based nanozymes with multifunctional attributes for biomedicine: expanding antioxidant therapeutics for neuroprotection, cancer, and anti-inflammatory pathologies. *Coord. Chem. Rev.* 469, 214685. doi:10.1016/j.ccr.2022.214685
- Lough, A. J. M., Connelly, D. P., Homoky, W. B., Hawkes, J. A., Chavagnac, V., Castillo, A., et al. (2019). Diffuse hydrothermal venting: a hidden source of iron to the oceans. *Front. Mar. Sci.* 6. doi:10.3389/fmars.2019.00329
- Lu, T., Wang, X., Cui, X., Li, J., Xu, J., Xu, P., et al. (2023). Physiological and metabolomic analyses reveal that Fe_3O_4 nanoparticles ameliorate cadmium and arsenic toxicity in Panax notoginseng. *Environ. Pollut.* 337, 122578. doi:10.1016/j.envpol.2023.122578
- Luo, H.-W., Zhang, X., Chen, J.-J., Yu, H.-Q., and Sheng, G.-P. (2017). Probing the biotransformation of hematite nanoparticles and magnetite formation mediated by *Shewanella oneidensis* MR-1 at the molecular scale. *Environ. Sci. Nano* 4, 2395–2404. doi:10.1039/c7en00767a
- Lyons, T. W., Reinhard, C. T., and Planavsky, N. J. (2014). The rise of oxygen in Earth's early ocean and atmosphere. *Nature* 506, 307–315. doi:10.1038/nature13068
- Ma, L., Zheng, J.-J., Zhou, N., Zhang, R., Fang, L., Yang, Y., et al. (2024). A natural biogenic nanozyme for scavenging superoxide radicals. *Nat. Commun.* 15, 233. doi:10.1038/s41467-023-44463-w
- Ma, Y., Tian, Z., Zhai, W., and Qu, Y. (2022). Insights on catalytic mechanism of CeO_2 as multiple nanozymes. *Nano Res.* 15, 10328–10342. doi:10.1007/s12274-022-4666-y
- Maher, B. A. (2016). Palaeoclimatic records of the loess/palaeosol sequences of the Chinese Loess Plateau. *Quat. Sci. Rev.* 154, 23–84. doi:10.1016/j.quascirev.2016.08.004
- Manceau, A., and Combes, J. M. (1988). Structure of Mn and Fe oxides and oxyhydroxides: a topological approach by EXAFS. *Phys. Chem. Min.* 15, 283–295. doi:10.1007/bf00307518
- Marcus, R. A., and Sutin, N. (1985). Electron transfers in chemistry and biology. *BBA Rev. Bioenergetics* 811, 265–322. doi:10.1016/0304-4173(85)90014-x
- Mcguinness, K. N., Klau, G. W., Morrison, S. M., Moore, E. K., Seipp, J., Falkowski, P. G., et al. (2022). Evaluating mineral lattices as evolutionary proxies for metalloprotein evolution. *Orig. Life Evol. Biosph.* 52, 263–275. doi:10.1007/s11084-022-09630-x
- Meng, X., Li, D., Chen, L., He, H., Wang, Q., Hong, C., et al. (2021). High-performance self-cascade pyrite nanozymes for apoptosis-ferroptosis synergistic tumor therapy. *ACS Nano* 15, 5735–5751. doi:10.1021/acsnano.1c01248
- Meng, Y., Li, W., Pan, X., and Gadd, G. M. (2020). Applications of nanozymes in the environment. *Environ. Sci. Nano* 7, 1305–1318. doi:10.1039/c9en01089k
- Messner, K. R., and Imlay, J. A. (2002). Mechanism of superoxide and hydrogen peroxide formation by fumarate reductase, succinate dehydrogenase, and aspartate oxidase. *J. Biol. Chem.* 277, 42563–42571. doi:10.1074/jbc.m204958200
- Michel, F. M., Barrón, V., Torrent, J., Morales, M. P., Serna, C. J., Boily, J. F., et al. (2010). Ordered ferrimagnetic form of ferrihydrite reveals links among structure, composition, and magnetism. *Proc. Natl. Acad. Sci. U. S. A.* 107, 2787–2792. doi:10.1073/pnas.0910170107
- Michel, F. M., Ehm, L., Antao, S. M., Lee, P. L., Chupas, P. J., Liu, G., et al. (2007). The structure of ferrihydrite, a nanocrystalline material. *Science* 316, 1726–1729. doi:10.1126/science.1142525
- Miller, S. L. (1953). A production of amino acids under possible primitive earth conditions. *Science* 117, 528–529. doi:10.1126/science.117.3046.528
- Milton, R. D., and Minteer, S. D. (2017). Direct enzymatic bioelectrocatalysis: differentiating between myth and reality. *J. R. Soc. Interface* 14, 20170253. doi:10.1098/rsif.2017.0253
- Mitchell, C. E., Terranova, U., Beale, A. M., Jones, W., Morgan, D. J., Sankar, M., et al. (2021). A surface oxidised Fe–S catalyst for the liquid phase hydrogenation of CO_2 . *Catal. Sci. Technol.* 11, 779–784. doi:10.1039/d0cy01779e
- Mitić, N., Smith, S. J., Neves, A., Guddat, L. W., Gahan, L. R., and Schenk, G. (2006). The catalytic mechanisms of binuclear metallohydrolases. *Chem. Rev.* 106, 3338–3363. doi:10.1021/cr050318f
- Montini, T., Melchiorre, M., Monai, M., and Fornasiero, P. (2016). Fundamentals and catalytic applications of CeO_2 -based materials. *Chem. Rev.* 116, 5987–6041. doi:10.1021/acs.chemrev.5b00603
- Morris, E. R., and Williams, Q. (1997). Electrical resistivity of Fe_3O_4 to 48 GPa: compression-induced changes in electron hopping at mantle pressures. *J. Geophys. Res. Solid Earth* 102, 18139–18148. doi:10.1029/97jb00024
- Mostajabi Sarhangi, S., and Matyushov, D. V. (2023). Electron tunneling in biology: when does it matter? *ACS Omega* 8, 27355–27365. doi:10.1021/acsomega.3c02719
- Mu, J., Wang, Y., Zhao, M., and Zhang, L. (2012). Intrinsic peroxidase-like activity and catalase-like activity of Co_3O_4 nanoparticles. *Chem. Commun.* 48, 2540–2542. doi:10.1039/c2cc17013b
- Mu, J., Zhang, L., Zhao, G., and Wang, Y. (2014). The crystal plane effect on the peroxidase-like catalytic properties of Co_3O_4 nanomaterials. *Phys. Chem. Chem. Phys.* 16, 15709–15716. doi:10.1039/c4cp01326c
- Natalio, F., André, R., Hartog, A. F., Stoll, B., Jochum, K. P., Wever, R., et al. (2012). Vanadium pentoxide nanoparticles mimic vanadium haloperoxidases and thwart biofilm formation. *Nat. Nanotechnol.* 7, 530–535. doi:10.1038/nnano.2012.91
- Navrotsky, A., Mazeina, L., and Majzlan, J. (2008). Size-driven structural and thermodynamic complexity in iron oxides. *Science* 319, 1635–1638. doi:10.1126/science.1148614
- Neubeck, A., and Freund, F. (2020). Sulfur chemistry may have paved the way for evolution of antioxidants. *Astrobiology* 20, 670–675. doi:10.1089/ast.2019.2156
- Nie, X., Xia, L., Wang, H.-L., Chen, G., Wu, B., Zeng, T.-Y., et al. (2019). Photothermal therapy nanomaterials boosting transformation of Fe(III) into Fe(II) in tumor cells for highly improving chemodynamic therapy. *ACS Appl. Mater. Interfaces* 11, 31735–31742. doi:10.1021/acsami.9b11291
- Nitschke, W., and Russell, M. J. (2009). Hydrothermal focusing of chemical and chemoisotropic energy, supported by delivery of catalytic Fe, Ni, Mo/W, Co, S and Se, forced life to emerge. *J. Mol. Evol.* 69, 481–496. doi:10.1007/s00239-009-9289-3
- Niu, X., Li, X., Lyu, Z., Pan, J., Ding, S., Ruan, X., et al. (2020). Metal–organic framework based nanozymes: promising materials for biochemical analysis. *Chem. Commun.* 56, 11338–11353. doi:10.1039/d0cc04890a
- Niu, X., Xu, X., Li, X., Pan, J., Qiu, F., Zhao, H., et al. (2018). Surface charge engineering of nanosized CuS via acidic amino acid modification enables high peroxidase-mimicking activity at neutral pH for one-pot detection of glucose. *Chem. Commun.* 54, 13443–13446. doi:10.1039/c8cc07800a
- Noh, J., Osman, O. I., Aziz, S. G., Winget, P., and Brédas, J.-L. (2015). Magnetite Fe_3O_4 (111) surfaces: impact of defects on structure, stability, and electronic properties. *Chem. Mat.* 27, 5856–5867. doi:10.1021/acs.chemmater.5b02885
- Ohta, K., Cohen, R. E., Hirose, K., Haule, K., Shimizu, K., and Ohishi, Y. (2012). Experimental and theoretical evidence for pressure-induced metallization in FeO with rocksalt-type structure. *Phys. Rev. Lett.* 108, 026403. doi:10.1103/physrevlett.108.026403
- Ohta, K., Hirose, K., Shimizu, K., and Ohishi, Y. (2010). High-pressure experimental evidence for metal FeO with normal NiAs-type structure. *Phys. Rev. B* 82, 174120. doi:10.1103/physrevb.82.174120
- Olson, K. R., Gao, Y., Deleon, E. R., Arif, M., Arif, F., Arora, N., et al. (2017). Catalase as a sulfide–sulfur oxido-reductase: an ancient (and modern?) regulator of reactive sulfur species (RSS). *Redox Biol.* 12, 325–339. doi:10.1016/j.redox.2017.02.021
- Oparin, A. I. (1938). *The origin of life*. New York: MacMillan.
- Oró, J. (1961). Mechanism of synthesis of adenine from hydrogen cyanide under possible primitive earth conditions. *Nature* 191, 1193–1194. doi:10.1038/1911193a0
- Ovsyannikov, S. V., Bykov, M., Bykova, E., Glazyrin, K., Manna, R. S., Tsirlin, A. A., et al. (2018). Pressure tuning of charge ordering in iron oxide. *Nat. Commun.* 9, 4142. doi:10.1038/s41467-018-06457-x
- Ovsyannikov, S. V., Bykov, M., Bykova, E., Kozlenko, D. P., Tsirlin, A. A., Karkin, A. E., et al. (2016). Charge-ordering transition in iron oxide Fe_4O_5 involving competing dimer and trimer formation. *Nat. Chem.* 8, 501–508. doi:10.1038/nchem.2478
- Ovsyannikov, S. V., Bykov, M., Medvedev, S. A., Naumov, P. G., Jesche, A., Tsirlin, A. A., et al. (2020). A room-temperature verwey-type transition in iron oxide, Fe_5O_6 . *Angew. Chem. Int. Ed.* 59, 5632–5636. doi:10.1002/anie.201914988
- Paidi, V. K., Shepit, M., Freeland, J. W., Brewe, D. L., Roberts, C. A., and Van Lierop, J. (2021). Intervening oxygen enabled magnetic moment modulation in spinel nanostructures. *J. Phys. Chem. C* 125, 26688–26697. doi:10.1021/acs.jpcc.1c06494

- Pan, Y., Li, N., Mu, J., Zhou, R., Xu, Y., Cui, D., et al. (2015). Biogenic magnetic nanoparticles from *Burkholderia* sp. YN01 exhibiting intrinsic peroxidase-like activity and their applications. *Appl. Microbiol. Biotechnol.* 99, 703–715. doi:10.1007/s00253-014-5938-6
- Pan, Y., Wang, Y., Fan, X., Wang, W., Yang, X., Cui, D., et al. (2019). Bacterial intracellular nanoparticles exhibiting antioxidant properties and the significance of their formation in ROS detoxification. *Environ. Microbiol. Rep.* 11, 140–146. doi:10.1111/1758-2229.12733
- Pasternak, M. P., Rozenberg, G. K., Machavariani, G. Y., Naaman, O., Taylor, R. D., and Jeanloz, R. (1999). Breakdown of the mott-hubbard state in Fe_2O_3 : a first-order insulator-metal transition with collapse of magnetism at 50 GPa. *Phys. Rev. Lett.* 82, 4663–4666. doi:10.1103/physrevlett.82.4663
- Patrick, R. a.D., Coker, V. S., Akhtar, M., Malik, M. A., Lewis, E., Haigh, S., et al. (2017). Magnetic spectroscopy of nanoparticulate greigite, Fe_3S_4 . *Mineral. Mag.* 81, 857–872. doi:10.1180/minmag.2016.080.114
- Peng, C., Jiang, B., Liu, Q., Guo, Z., Xu, Z., Huang, Q., et al. (2011). Graphene-templated formation of two-dimensional lepidocrocite nanostructures for high-efficiency catalytic degradation of phenols. *Energy Environ. Sci.* 4, 2035–2040. doi:10.1039/c0ee00495b
- Peng, Y., Wang, Z., Liu, W., Zhang, H., Zuo, W., Tang, H., et al. (2015). Size- and shape-dependent peroxidase-like catalytic activity of MnFe_2O_4 Nanoparticles and their applications in highly efficient colorimetric detection of target cancer cells. *Dalton Trans.* 44, 12871–12877. doi:10.1039/c5dt01585e
- Peter, Y., and Theodore, K. (1977). Reversible electrode reaction of cytochrome C. *Chem. Lett.* 6, 1145–1148. doi:10.1246/cl.1977.1145
- Pham, H. H., Cheng, M.-J., Frei, H., and Wang, L.-W. (2016). Surface proton hopping and fast-kinetics pathway of water oxidation on Co_3O_4 (001) surface. *ACS Catal.* 6, 5610–5617. doi:10.1021/ascata.6b00713
- Poole, L. B. (1996). Flavin-dependent alkyl hydroperoxide reductase from *Salmonella typhimurium*. 2. Cystine disulfides involved in catalysis of peroxide reduction. *Biochemistry* 35, 65–75. doi:10.1021/bi951888k
- Pósfai, M., Lefèvre, C., Trubitsyn, D., Bazylinski, D., and Frankel, R. (2013). Phylogenetic significance of composition and crystal morphology of magnetosome minerals. *Front. Microbiol.* 4, 344. doi:10.3389/fmicb.2013.00344
- Posth, N. R., Canfield, D. E., and Kappler, A. (2014). Biogenic Fe(III) minerals: from formation to diagenesis and preservation in the rock record. *Earth-Sci. Rev.* 135, 103–121. doi:10.1016/j.earscirev.2014.03.012
- Potiszil, C., Ota, T., Yamamoto, M., Sakaguchi, C., Kobayashi, K., Tanaka, R., et al. (2023). Insights into the formation and evolution of extraterrestrial amino acids from the asteroid Ryugu. *Nat. Commun.* 14, 1482. doi:10.1038/s41467-023-37107-6
- Puvvada, N., Panigrahi, P. K., Mandal, D., and Pathak, A. (2012). Shape dependent peroxidase mimetic activity towards oxidation of pyrogallol by H_2O_2 . *RSC Adv.* 2, 3270–3273. doi:10.1039/c2ra01081j
- Pyle, A. M. (1993). Ribozymes: a distinct class of metalloenzymes. *Science* 261, 709–714. doi:10.1126/science.7688142
- Qi, Y., Sun, Y., Song, D., Wang, Y., and Xiu, F. (2023). PVC dechlorination residues as new peroxidase-mimicking nanzyme and chemiluminescence sensing probe with high activity for glucose and ascorbic acid detection. *Talanta* 253, 124039. doi:10.1016/j.talanta.2022.124039
- Qiao, F., Chen, L., Li, X., Li, L., and Ai, S. (2014). Peroxidase-like activity of manganese selenide nanoparticles and its analytical application for visual detection of hydrogen peroxide and glucose. *Sens. Actuators B Chem.* 193, 255–262. doi:10.1016/j.snb.2013.11.108
- Qin, T., Ma, R., Yin, Y., Miao, X., Chen, S., Fan, K., et al. (2019). Catalytic inactivation of influenza virus by iron oxide nanzyme. *Theranostics* 9, 6920–6935. doi:10.7150/thno.35826
- Qiu, H., Xu, T., Wang, Z., Ren, W., Nan, H., Ni, Z., et al. (2013). Hopping transport through defect-induced localized states in molybdenum disulphide. *Nat. Commun.* 4, 2642. doi:10.1038/ncomms3642
- Raanan, H., Poudel, S., Pike, D. H., Nanda, V., and Falkowski, P. G. (2020). Small protein folds at the root of an ancient metabolic network. *Proc. Natl. Acad. Sci. U. S. A.* 117, 7193–7199. doi:10.1073/pnas.1914982117
- Radisavljevic, B., Radenovic, A., Brivio, J., Giacometti, V., and Kis, A. (2011). Single-layer MoS₂ transistors. *Nat. Nanotechnol.* 6, 147–150. doi:10.1038/nnano.2010.279
- Radoń, A., Łukowicz, D., Kremzer, M., Mikula, J., and Włodarczyk, P. (2018). Electrical conduction mechanism and dielectric properties of spherical shaped Fe_3O_4 nanoparticles synthesized by Co-precipitation method. *Materials* 11, 735. doi:10.3390/ma11050735
- Ragg, R., Natalio, F., Tahir, M. N., Janssen, H., Kashyap, A., Strand, D., et al. (2014). Molybdenum trioxide nanoparticles with intrinsic sulfite oxidase activity. *ACS Nano* 8, 5182–5189. doi:10.1021/nm501235j
- Raiswell, R., and Canfield, D. E. (2012). The iron biogeochemical cycle past and present. *Geochem. Perspect.* 1, 1–220. doi:10.7185/geochempersp.1.1
- Ratautas, D., and Dagys, M. (2020). Nanocatalysts containing direct electron transfer-capable oxidoreductases: recent advances and applications. *Catalysts* 10, 9. doi:10.3390/catal10010009
- Rebelein, J. G., Hu, Y., and Ribbe, M. W. (2015). Widening the product profile of carbon dioxide reduction by vanadium nitrogenase. *ChemBioChem* 16, 1993–1996. doi:10.1002/cbic.201500305
- Ren, H., Yong, J., Yang, Q., Yang, Z., Liu, Z., Xu, Y., et al. (2021). Self-assembled FeS-based cascade bioreactor with enhanced tumor penetration and synergistic treatments to trigger robust cancer immunotherapy. *Acta Pharm. Sin. B* 11, 3244–3261. doi:10.1016/j.apsb.2021.05.005
- Reyda, M. R., Fugate, C. J., and Jarrett, J. T. (2009). A complex between biotin synthase and the iron-sulfur cluster assembly chaperone HscA that enhances *in vivo* cluster assembly. *Biochemistry* 48, 10782–10792. doi:10.1021/bi901393t
- Rickard, D., and Luther, G. W. (2007). Chemistry of iron sulfides. *Chem. Rev.* 107, 514–562. doi:10.1021/cr0503658
- Rizwan, M., Noureen, S., Ali, S., Anwar, S., Rehman, M. Z., Qayyum, M. F., et al. (2019). Influence of biochar amendment and foliar application of iron oxide nanoparticles on growth, photosynthesis, and cadmium accumulation in rice biomass. *J. Soils Sediments* 19, 3749–3759. doi:10.1007/s11368-019-02327-1
- Roberts, D. M., Landin, A. R., Ritter, T. G., Eaves, J. D., and Stoldt, C. R. (2018). Nanocrystalline iron monosulfides near stoichiometry. *Sci. Rep.* 8, 6591. doi:10.1038/s41598-018-24739-8
- Rodríguez-López, J. N., Lowe, D. J., Hernández-Ruiz, J., Hiner, A. N., García-Cánovas, F., and Thorneley, R. N. (2001). Mechanism of reaction of hydrogen peroxide with horseradish peroxidase: identification of intermediates in the catalytic cycle. *J. Am. Chem. Soc.* 123, 11838–11847. doi:10.1021/ja011853+
- Roldan, A., Santos-Carballal, D., and De Leeuw, N. H. (2013). A comparative DFT study of the mechanical and electronic properties of greigite Fe_3S_4 and magnetite Fe_3O_4 . *J. Chem. Phys.* 138, 204712. doi:10.1063/1.4807614
- Runnegar, B. (1991). Precambrian oxygen levels estimated from the biochemistry and physiology of early eukaryotes. *Glob. Planet. Change* 5, 97–111. doi:10.1016/0921-8181(91)90131-f
- Russell, M. J. (2023). A self-sustaining serpentinization mega-engine feeds the fougere nanoengines implicated in the emergence of guided metabolism. *Front. Microbiol.* 14, 1145915. doi:10.3389/fmicb.2023.1145915
- Russell, M. J., and Hall, A. J. (1997). The emergence of life from iron monosulphide bubbles at a submarine hydrothermal redox and pH front. *J. Geol. Soc. Lond.* 154, 377–402. doi:10.1144/gsjgs.154.3.0377
- Russell, M. J., Hall, A. J., and Martin, W. (2010). Serpentinization as a source of energy at the origin of life. *Geobiology* 8, 355–371. doi:10.1111/j.1472-4669.2010.00249.x
- Sagnotti, L. (2007). “Iron sulfides,” in *Encyclopedia of geomagnetism and paleomagnetism*. Editors D. Gubbins, and E. Herrero-Bervera (Dordrecht: Springer Netherlands), 454–459.
- Sakkopoulos, S., Vitoratos, E., and Argyreas, T. (1984). Energy-band diagram for pyrrhotite. *J. Phys. Chem. Solids* 45, 923–928. doi:10.1016/0022-3697(84)90135-5
- Sanchez, C., Babonneau, F., Morineau, R., Livage, J., and Bullot, J. (1983a). Semiconducting properties of V_2O_5 gels. *Philos. Mag. B* 47, 279–290. doi:10.1080/13642812.1983.9728310
- Sanchez, C., Morineau, R., and Livage, J. (1983b). Electrical conductivity of amorphous V_2O_5 . *Phys. status solidi (a)* 76, 661–666. doi:10.1002/pssa.2210760232
- Sarraf, M., Vishwakarma, K., Kumar, V., Arif, N., Das, S., Johnson, R., et al. (2022). Metal/metalloid-based nanomaterials for plant abiotic stress tolerance: an overview of the mechanisms. *Plants* 11, 316. doi:10.3390/plants11030316
- Schenk, G., Mitić, N., Hanson, G. R., and Comba, P. (2013). Purple acid phosphatase: a journey into the function and mechanism of a colorful enzyme. *Coord. Chem. Rev.* 257, 473–482. doi:10.1016/j.ccr.2012.03.020
- Seino, H., and Hidai, M. (2011). Catalytic functions of cubane-type M_4S_4 clusters. *Chem. Sci.* 2, 847–857. doi:10.1039/c0sc00545b
- Senn, M. S., Wright, J. P., and Attfield, J. P. (2012). Charge order and three-site distortions in the Verwey structure of magnetite. *Nature* 481, 173–176. doi:10.1038/nature10704
- Sephton, M. A., and Botta, O. (2008). Extraterrestrial organic matter and the detection of life. *Space Sci. Rev.* 135, 25–35. doi:10.1007/s11214-007-9171-9
- Sepunaru, L., Refaelly-Abramson, S., Lovrinčić, R., Gavrilov, Y., Agrawal, P., Levy, Y., et al. (2015). Electronic transport via homopeptides: the role of side chains and secondary structure. *J. Am. Chem. Soc.* 137, 9617–9626. doi:10.1021/jacs.5b03933
- Setvin, M., Franchini, C., Hao, X., Schmid, M., Janotti, A., Kaltak, M., et al. (2014). Direct view at excess electrons in TiO_2 rutile and anatase. *Phys. Rev. Lett.* 113, 086402. doi:10.1103/physrevlett.113.086402
- Shan, Y., Lu, W., Xi, J., and Qian, Y. (2022). Biomedical applications of iron sulfide-based nanzymes. *Front. Chem.* 10, 1000709. doi:10.3389/fchem.2022.1000709
- Sharma, P., Jha, A. B., Dubey, R. S., and Pessarakli, M. (2012). Reactive oxygen species, oxidative damage, and antioxidative defense mechanism in plants under stressful conditions. *J. Bot.* 2012, 1–26. doi:10.1155/2012/217037
- Sheng, Y., Abreu, I. A., Cabelli, D. E., Maroney, M. J., Miller, A. F., Teixeira, M., et al. (2014). Superoxide dismutases and superoxide reductases. *Chem. Rev.* 114, 3854–3918. doi:10.1021/cr4005296

- Shleev, S., Tkac, J., Christenson, A., Ruzgas, T., Yaropolov, A. I., Whittaker, J. W., et al. (2005). Direct electron transfer between copper-containing proteins and electrodes. *Biosens. Bioelectron.* 20, 2517–2554. doi:10.1016/j.bios.2004.10.003
- Shu, Z., Liu, L., Tan, W., Suib, S. L., Qiu, G., Yang, X., et al. (2019). Solar irradiation induced transformation of ferrihydrite in the presence of aqueous Fe²⁺. *Environ. Sci. Technol.* 53, 8854–8861. doi:10.1021/acs.est.9b02750
- Shu, Z., Pan, Z., Wang, X., He, H., Yan, S., Zhu, X., et al. (2022). Sunlight-induced interfacial electron transfer of ferrihydrite under oxic conditions: mineral transformation and redox active species production. *Environ. Sci. Technol.* 56, 14188–14197. doi:10.1021/acs.est.2c04594
- Sidorov, N. S., Palnichenko, A. V., and Khasanov, S. S. (2011). Superconductivity in the metallic-oxidized copper interface. *Phys. C Supercond.* 471, 247–249. doi:10.1016/j.physc.2011.02.006
- Sies, H. (2017). Hydrogen peroxide as a central redox signaling molecule in physiological oxidative stress: oxidative eustress. *Redox Biol.* 11, 613–619. doi:10.1016/j.redox.2016.12.035
- Singh, K., Guju, R., Bandaru, S., Misra, S., Babu, K. S., and Puvvada, N. (2022). Facet-Dependent bactericidal activity of Ag₃PO₄ nanostructures against gram-positive/negative bacteria. *ACS Omega* 7, 16616–16628. doi:10.1021/acsomega.2c00864
- Singh, S. (2019). Nanomaterials exhibiting enzyme-like properties (nanozymes): current advances and future perspectives. *Front. Chem.* 7, 46. doi:10.3389/fchem.2019.00046
- Skomurski, F. N., Kerisit, S., and Rosso, K. M. (2010). Structure, charge distribution, and electron transfer dynamics in magnetite (Fe₃O₄) (100) surfaces from first principles. *Geochim. Cosmochim. Acta* 74, 4234–4248. doi:10.1016/j.gca.2010.04.063
- Slesak, I., Libik, M., Karpinska, B., Karpinski, S., and Miszalski, Z. (2007). The role of hydrogen peroxide in regulation of plant metabolism and cellular signalling in response to environmental stresses. *Acta Biochim. Pol.* 54, 39–50. doi:10.18388/abp.2007_3267
- Slesak, I., Slesak, H., and Kruk, J. (2012). Oxygen and hydrogen peroxide in the early evolution of life on earth: *in silico* comparative analysis of biochemical pathways. *Astrobiology* 12, 775–784. doi:10.1089/ast.2011.0704
- Slesak, I., Slesak, H., Zimak-Piekarczyk, P., and Rozpadek, P. (2016). Enzymatic antioxidant systems in early anaerobes: theoretical considerations. *Astrobiology* 16, 348–358. doi:10.1089/ast.2015.1328
- Solomon, E. I., Randall, D. W., and Glaser, T. (2000). Electronic structures of active sites in electron transfer metalloproteins: contributions to reactivity. *Coord. Chem. Rev.* 200–202, 595–632. doi:10.1016/s0010-8545(00)00332-5
- Song, C., Liu, H., Zhang, L., Wang, J., Zhao, C., Xu, Q., et al. (2022). FeS nanoparticles embedded in 2D carbon nanosheets as novel nanozymes with peroxidase-like activity for colorimetric and fluorescence assay of H₂O₂ and antioxidant capacity. *Sens. Actuators B Chem.* 353, 131131. doi:10.1016/j.snb.2021.131131
- Span, I., Wang, K., Wang, W., Zhang, Y., Bacher, A., Eisenreich, W., et al. (2012). Discovery of acetylene hydratase activity of the iron-sulphur protein lspH. *Nat. Commun.* 3, 1042. doi:10.1038/ncomms2052
- Stokkermans, J. P., Pierik, A. J., Wolbert, R. B., Hagen, W. R., Van Dongen, W. M., and Veeger, C. (1992). The primary structure of a protein containing a putative [6Fe-6S] prisme cluster from Desulfovibrio vulgaris (Hildenborough). *Eur. J. Biochem.* 208, 435–442. doi:10.1111/j.1432-1033.1992.tb17205.x
- Stone, J., Edgar, J. O., Gould, J. A., and Telling, J. (2022). Tectonically-driven oxidant production in the hot biosphere. *Nat. Commun.* 13, 4529. doi:10.1038/s41467-022-32129-y
- Subramani, T., Lilova, K., Abramchuk, M., Leinenweber, K. D., and Navrotsky, A. (2020). Greigite (Fe₃S₄) is thermodynamically stable: implications for its terrestrial and planetary occurrence. *Proc. Natl. Acad. Sci. U. S. A.* 117, 28645–28648. doi:10.1073/pnas.2017312117
- Sun, D., Liu, T., Dong, Y., Liu, Q., Wu, X., and Wang, G.-L. (2021). Coupling p-hydroxybenzoate hydroxylase with the photoresponsive nanozyme for universal dehydrogenase-based bioassays. *Sens. Actuators B Chem.* 327, 128859. doi:10.1016/j.snb.2020.128859
- Suprun, E. V. (2021). Direct electrochemistry of proteins and nucleic acids: the focus on 3D structure. *Electrochim Commun.* 125, 106983. doi:10.1016/j.electcom.2021.106983
- Suri, D., and Patel, R. S. (2017). Electron and thermal transport via variable range hopping in MoSe₂ single crystals. *Appl. Phys. Lett.* 110, 233108. doi:10.1063/1.4984953
- Takele, S., and Hearne, G. R. (1999). Electrical transport, magnetism, and spin-state configurations of high-pressure phases of FeS. *Phys. Rev. B* 60, 4401–4403. doi:10.1103/physrevb.60.4401
- Tamura, H., Tanaka, A., Mita, K.-Y., and Furuichi, R. (1999). Surface hydroxyl site densities on metal oxides as a measure for the ion-exchange capacity. *J. Colloid Interface Sci.* 209, 225–231. doi:10.1006/jcis.1998.5877
- Tan, Z., Chen, Y.-C., Zhang, J., Chou, J.-P., Hu, A., and Peng, Y.-K. (2020a). Nanoenzymes: the origin behind pristine CeO₂ as enzyme mimetics. *Chem. Eur. J.* 26, 10598–10606. doi:10.1002/chem.202001597
- Tan, Z., Wu, T.-S., Soo, Y.-L., and Peng, Y.-K. (2020b). Unravelling the true active site for CeO₂-catalyzed dephosphorylation. *Appl. Catal. B* 264, 118508. doi:10.1016/j.apcatb.2019.118508
- Tang, M., Zhang, Z., Sun, T., Li, B., and Wu, Z. (2022). Manganese-based nanozymes: preparation, catalytic mechanisms, and biomedical applications. *Adv. Healthc. Mat.* 11, 2201733. doi:10.1002/adhm.202201733
- Tang, Z., Wu, H., Zhang, Y., Li, Z., and Lin, Y. (2011). Enzyme-mimic activity of ferric nano-core residing in ferritin and its biosensing applications. *Anal. Chem.* 83, 8611–8616. doi:10.1021/ac202049q
- Tarashevich, M. R., Yaropolov, A. I., Bogdanovskaya, V. A., and Varfolomeev, S. D. (1979). Electrocatalysis of a cathodic oxygen reduction by laccase. *J. Electroanal. Chem.* 104, 393–403. doi:10.1016/s0022-0728(79)81047-5
- Taverne, Y. J., Caron, A., Diamond, C., Fournier, G., and Lyons, T. W. (2020). “Chapter 5 - oxidative stress and the early coevolution of life and biospheric oxygen,” in *Oxidative stress*. Editor H. Sies (Academic Press), 67–85.
- Taverne, Y. J., Merkus, D., Bogers, A. J., Halliwell, B., Duncker, D. J., and Lyons, T. W. (2018). Reactive oxygen species: radical factors in the evolution of animal life: a molecular timescale from earth’s earliest history to the rise of complex life. *Bioessays* 40, 1700158. doi:10.1002/bies.201700158
- Todo, S., Takeshita, N., Kanehara, T., Mori, T., and Mori, N. (2001). Metallization of magnetite (Fe₃O₄) under high pressure. *J. Appl. Phys.* 89, 7347–7349. doi:10.1063/1.1359460
- Tuller, H. L., and Nowick, A. S. (1977). Small polaron electron transport in reduced CeO₂ single crystals. *J. Phys. Chem. Solids* 38, 859–867. doi:10.1016/0022-3697(77)90124-x
- Uebel, R., and Schüller, D. (2016). Magnetosome biogenesis in magnetotactic bacteria. *Nat. Rev. Microbiol.* 14, 621–637. doi:10.1038/nrmicro.2016.99
- Usman, M., Abdelmoula, M., Hanna, K., Grégoire, B., Faure, P., and Ruby, C. (2012). FeII induced mineralogical transformations of ferric oxyhydroxides into magnetite of variable stoichiometry and morphology. *J. Solid State Chem.* 194, 328–335. doi:10.1016/j.jssc.2012.05.022
- Usman, M., Byrne, J. M., Chaudhary, A., Orsetti, S., Hanna, K., Ruby, C., et al. (2018). Magnetite and green rust: synthesis, properties, and environmental applications of mixed-valent iron minerals. *Chem. Rev.* 118, 3251–3304. doi:10.1021/acs.chemrev.7b00224
- Valko, M., Leibfritz, D., Moncol, J., Cronin, M. T. D., Mazur, M., and Telser, J. (2007). Free radicals and antioxidants in normal physiological functions and human disease. *Int. J. Biochem. Cell Biol.* 39, 44–84. doi:10.1016/j.biocel.2006.07.001
- Vallabani, N. V. S., Vinu, A., Singh, S., and Karakoti, A. (2020). Tuning the ATP-triggered pro-oxidant activity of iron oxide-based nanozyme towards an efficient antibacterial strategy. *J. Colloid Interface Sci.* 567, 154–164. doi:10.1016/j.jcis.2020.01.099
- Veitch, N. C. (2004). Horseradish peroxidase: a modern view of a classic enzyme. *Phytochemistry* 65, 249–259. doi:10.1016/j.phytochem.2003.10.022
- Verwey, E. J. W. (1939). Electronic conduction of magnetite (Fe₃O₄) and its transition point at low temperatures. *Nature* 144, 327–328. doi:10.1038/144327b0
- Wächtershäuser, G. (1988). Before enzymes and templates: theory of surface metabolism. *Microbiol. Rev.* 52, 452–484. doi:10.1128/mr.52.4.452-484.1988
- Wächtershäuser, G. (1990). Evolution of the first metabolic cycles. *Proc. Natl. Acad. Sci. U. S. A.* 87, 200–204. doi:10.1073/pnas.87.1.200
- Wächtershäuser, G. (1992). Groundworks for an evolutionary biochemistry: the iron-sulphur world. *Prog. Biophys. Mol. Biol.* 58, 85–201. doi:10.1016/0079-6107(92)90022-x
- Wander, M. C. F., Rosso, K. M., and Schoonen, M. a.A. (2007). Structure and charge hopping dynamics in green rust. *J. Phys. Chem. C* 111, 11414–11423. doi:10.1021/jp072762n
- Wang, H., and Huang, Y. (2011). Prussian-blue-modified iron oxide magnetic nanoparticles as effective peroxidase-like catalysts to degrade methylene blue with H₂O₂. *J. Hazard. Mat.* 191, 163–169. doi:10.1016/j.jhazmat.2011.04.057
- Wang, Q., Chen, J., Zhang, H., Wu, W., Zhang, Z., and Dong, S. (2018). Porous Co₃O₄ nanoplates with pH-switchable peroxidase- and catalase-like activity. *Nanoscale* 10, 19140–19146. doi:10.1039/c8nr06162a
- Wang, S., Wang, X., Du, B., Jin, Y., Ai, W., Zhang, G., et al. (2023). Hydrogen peroxide-assisted and histidine-stabilized copper-containing nanozyme for efficient degradation of various organic dyes. *Spectrochim. Acta A Mol. Biomol. Spectrosc.* 287, 122084. doi:10.1016/j.saa.2022.122084
- Wang, W., Yang, B., Qu, Y., Liu, X., and Su, W. (2011). FeS/FeS₂ redox system and its oxidoreductase-like chemistry in the iron-sulfur world. *Astrobiology* 11, 471–476. doi:10.1089/ast.2011.0624
- Wang, Y., Shen, X., Ma, S., Guo, Q., Zhang, W., Cheng, L., et al. (2020). Oral biofilm elimination by combining iron-based nanozymes and hydrogen peroxide-producing bacteria. *Biomater. Sci.* 8, 2447–2458. doi:10.1039/c9bm01889a
- Warren, J. J., Ener, M. E., Vlček, A., Jr., Winkler, J. R., and Gray, H. B. (2012). Electron hopping through proteins. *Coord. Chem. Rev.* 256, 2478–2487. doi:10.1016/j.ccr.2012.03.032

- Waser, V., Mukherjee, M., Tachibana, R., Igareta, N. V., and Ward, T. R. (2023). An artificial [Fe4S4]-containing metalloenzyme for the reduction of CO₂ to hydrocarbons. *J. Am. Chem. Soc.* 145, 14823–14830. doi:10.1021/jacs.3c03546
- Wei, H., Li, G., and Li, J. (2023). *Biomedical nanozymes, from diagnostics to therapeutics*. Singapore: Springer Singapore.
- Wei, H., and Wang, E. (2013). Nanomaterials with enzyme-like characteristics (nanozymes): Next-generation artificial enzymes. *Chem. Soc. Rev.* 42, 6060–6093. doi:10.1039/c3cs35486e
- Weiss, M. C., Sousa, F. L., Mrnjavac, N., Neukirchen, S., Roettger, M., Nelson-Sathi, S., et al. (2016). The physiology and habitat of the last universal common ancestor. *Nat. Microbiol.* 1, 16116. doi:10.1038/nm microbiol.2016.116
- Westall, F., and Southam, G. (2006). “The early record of life,” in *Archean geodynamics and environments*. Editors K. Benn, J.-C. Mareschal, and K. C. Condie (American Geophysical Union Geophysical Monograph), 283–304.
- White, L. M., Bhartia, R., Stucky, G. D., Kanik, I., and Russell, M. J. (2015). Mackinawite and greigite in ancient alkaline hydrothermal chimneys: identifying potential key catalysts for emergent life. *Earth Planet. Sci. Lett.* 430, 105–114. doi:10.1016/j.epsl.2015.08.013
- White, L. M., Shibuya, T., Vance, S. D., Christensen, L. E., Bhartia, R., Kidd, R., et al. (2020). Simulating serpentinization as it could apply to the emergence of life using the JPL hydrothermal reactor. *Astrobiology* 20, 307–326. doi:10.1089/ast.2018.1949
- Williams, R. J. P. (1981). Natural selection of the chemical elements. *Proc. R. Soc. B* 213, 361–397. doi:10.1098/rspb.1981.0071
- Williams, R. J. P. (2003). Metallo-enzyme catalysis. *Chem. Commun.* 3, 1109–1113. doi:10.1039/b211281g
- Woese, C. R., Kandler, O., and Wheelis, M. L. (1990). Towards a natural system of organisms: proposal for the domains Archaea, Bacteria, and Eucarya. *Proc. Natl. Acad. Sci. U. S. A.* 87, 4576–4579. doi:10.1073/pnas.87.12.4576
- Wong, E. L. S., Vuong, K. Q., and Chow, E. (2021). Nanozymes for environmental pollutant monitoring and remediation. *Sensors* 21, 408. doi:10.3390/s21020408
- Wu, J., Wang, X., Wang, Q., Lou, Z., Li, S., Zhu, Y., et al. (2019a). Nanomaterials with enzyme-like characteristics (nanozymes): Next-generation artificial enzymes (II). *Chem. Soc. Rev.* 48, 1004–1076. doi:10.1039/c8cs00457a
- Wu, W., Wang, Q., Chen, J., Huang, L., Zhang, H., Rong, K., et al. (2019b). Biomimetic design for enhancing the peroxidase mimicking activity of hemin. *Nanoscale* 11, 12603–12609. doi:10.1039/c9nr03506k
- Wu, X., Chen, T., Wang, J., and Yang, G. (2017). Few-layered MoSe₂ nanosheets as an efficient peroxidase nanozyme for highly sensitive colorimetric detection of H₂O₂ and xanthine. *J. Mater. Chem. B* 6, 105–111. doi:10.1039/c7tb02434g
- Wu, Z. Y., Gota, S., Jollet, F., Pollak, M., Gautier-Soyer, M., and Natoli, C. R. (1997). Characterization of iron oxides by x-ray absorption at the oxygen K edge using a full multiple-scattering approach. *Phys. Rev. B* 55, 2570–2577. doi:10.1103/physrevb.55.2570
- Xiao, G., Li, H., Zhao, Y., Wei, H., Li, J., and Su, H. (2022). Nanoceria-based artificial nanozymes: review of materials and applications. *ACS Appl. Nano Mater.* 5, 14147–14170. doi:10.1021/acsnano.2c03009
- Xie, W., Guo, Z., Gao, F., Gao, Q., Wang, D., Liaw, B. S., et al. (2018). Shape-size- and structure-controlled synthesis and biocompatibility of iron oxide nanoparticles for magnetic theranostics. *Theranostics* 8, 3284–3307. doi:10.7150/thno.25220
- Xu, D., Wu, L., Yao, H., and Zhao, L. (2022a). Catalase-like nanozymes: classification, catalytic mechanisms, and their applications. *Small* 18, 2203400. doi:10.1002/smll.202203400
- Xu, W., He, W., Du, Z., Zhu, L., Huang, K., Lu, Y., et al. (2021a). Functional nucleic acid nanomaterials: development, properties, and applications. *Angew. Chem. Int. Ed.* 60, 6890–6918. doi:10.1002/anie.201909927
- Xu, Z., Qiu, Z., Liu, Q., Huang, Y., Li, D., Shen, X., et al. (2018). Converting organosulfur compounds to inorganic polysulfides against resistant bacterial infections. *Nat. Commun.* 9, 3713. doi:10.1038/s41467-018-06164-7
- Xu, Z., Qu, A., Wang, W., Lu, M., Shi, B., Chen, C., et al. (2021b). Facet-Dependent biodegradable Mn₃O₄ nanoparticles for ameliorating Parkinson’s disease. *Adv. Healthc. Mat.* 10, 2101316. doi:10.1002/adhm.202101316
- Xu, Z. F., Tong, C. J., Si, R. T., Teobaldi, G., and Liu, L. M. (2022b). Nonadiabatic dynamics of polaron hopping and coupling with water on reduced TiO₂. *J. Phys. Chem. Lett.* 13, 857–863. doi:10.1021/acs.jpclett.1c04231
- Yang, W., Yang, X., Zhu, L., Chu, H., Li, X., and Xu, W. (2021). Nanozymes: activity origin, catalytic mechanism, and biological application. *Coord. Chem. Rev.* 448, 214170. doi:10.1016/j.ccr.2021.214170
- Yang, Y., Mao, Z., Huang, W., Liu, L., Li, J., Li, J., et al. (2016a). Redox enzyme-mimicking activities of CeO₂ nanostructures: intrinsic influence of exposed facets. *Sci. Rep.* 6, 35344. doi:10.1038/srep35344
- Yang, Y., Vance, M., Tou, F., Tiwari, A., Liu, M., and Hochella, M. F. (2016b). Nanoparticles in road dust from impervious urban surfaces: distribution, identification, and environmental implications. *Environ. Sci. Nano* 3, 534–544. doi:10.1039/c6en00056h
- Yao, W. T., Zhu, H. Z., Li, W. G., Yao, H. B., Wu, Y. C., and Yu, S. H. (2013). Intrinsic peroxidase catalytic activity of Fe₃S₈ nanowires templated from [Fe₁₆S₂₀]/diethylenetriamine hybrid nanowires. *ChemPlusChem* 78, 723–727. doi:10.1002/cplu.201300075
- Yaropolov, A. I., Malovik, V., Varfolomeyev, S. D., and Berezin, I. V. (1979). Electroreduction of hydrogen peroxide on an electrode with immobilized peroxidase. *Dokl. Akad. Nauk. SSSR* 249, 1399.
- Yu, X., Huo, C. F., Li, Y. W., Wang, J., and Jiao, H. (2012). Fe₃O₄ surface electronic structures and stability from GGA+U. *Surf. Sci.* 606, 872–879. doi:10.1016/j.susc.2012.02.003
- Yu, Y., Lu, L., Yang, Q., Zupanic, A., Xu, Q., and Jiang, L. (2021). Using MoS₂ nanomaterials to generate or remove reactive oxygen species: a review. *ACS Appl. Nano Mater* 4, 7523–7537. doi:10.1021/acsannm.1c00751
- Yuan, Y., Wang, L., and Gao, L. (2020). Nano-sized iron sulfide: structure, synthesis, properties, and biomedical applications. *Front. Chem.* 8, 818. doi:10.3389/fchem.2020.00818
- Yücel, M., Sevgen, S., and Le Bris, N. (2021). Soluble, colloidal, and particulate iron across the hydrothermal vent mixing zones in broken spur and Rainbow, mid-atlantic ridge. *Front. Microbiol.* 12, 631885. doi:10.3389/fmicb.2021.631885
- Zámocký, M., Gasselhuber, B., Furtmüller, P. G., and Obinger, C. (2012). Molecular evolution of hydrogen peroxide degrading enzymes. *Arch. Biochem. Biophys.* 525, 131–144. doi:10.1016/j.abb.2012.01.017
- Zanella, D., Bossi, E., Gornati, R., Bastos, C., Faria, N., and Bernardini, G. (2017). Iron oxide nanoparticles can cross plasma membranes. *Sci. Rep.* 7, 11413. doi:10.1038/s41598-017-11535-z
- Zarzycki, P., Smith, D. M., and Rosso, K. M. (2015). Proton dynamics on goethite nanoparticles and coupling to electron transport. *J. Chem. Theory Comput.* 11, 1715–1724. doi:10.1021/ct500891a
- Zelko, I. N., Mariani, T. J., and Folz, R. J. (2002). Superoxide dismutase multigene family: a comparison of the CuZn-SOD (SOD1), Mn-SOD (SOD2), and EC-SOD (SOD3) gene structures, evolution, and expression. *Free Radic. Biol. Med.* 33, 337–349. doi:10.1016/s0891-5849(02)00905-x
- Zhang, J., Li, S., Xie, N., Nie, G., Tang, A., Zhang, X. E., et al. (2021a). A natural nanozyme in life is found: the iron core within ferritin shows superoxide dismutase catalytic activity. *Sci. China Life Sci.* 64, 1375–1378. doi:10.1007/s11427-020-1865-2
- Zhang, L., Han, L., Hu, P., Wang, L., and Dong, S. (2013). TiO₂ nanotube arrays: intrinsic peroxidase mimetics. *Chem. Commun.* 49, 10480–10482. doi:10.1039/c3cc46163g
- Zhang, R., Chen, L., Liang, Q., Xi, J., Zhao, H., Jin, Y., et al. (2021b). Unveiling the active sites on ferrihydrite with apparent catalase-like activity for potentiating radiotherapy. *Nano Today* 41, 101317. doi:10.1016/j.nantod.2021.101317
- Zhang, R., Zhao, H., and Fan, K. (2022). “Structure-activity mechanism of iron oxide nanozymes,” in *Nanozymes: design, synthesis, and applications* (American Chemical Society), 1–35.
- Zhang, X., Li, G., Chen, G., Wu, D., Wu, Y., and James, T. D. (2021c). Enzyme mimics for engineered biomimetic cascade nanoreactors: mechanism, applications, and prospects. *Adv. Funct. Mat.* 31, 2106139. doi:10.1002/adfm.202106139
- Zhang, Y., Wang, Z., Li, X., Wang, L., Yin, M., Wang, L., et al. (2016). Dietary iron oxide nanoparticles delay aging and ameliorate neurodegeneration in *Drosophila*. *Adv. Mater* 28, 1387–1393. doi:10.1002/adma.201503893
- Zhao, D., Barlett, S., and Yung, Y. L. (2020). Quantifying mineral-ligand structural similarities: bridging the geological world of minerals with the biological world of enzymes. *Life* 10, 338–339. doi:10.3390/life10120338
- Zhao, H., Zhang, R., Yan, X., and Fan, K. (2021). Superoxide dismutase nanozymes: an emerging star for anti-oxidation. *J. Mater. Chem. B* 9, 6939–6957. doi:10.1039/d1tb00720c
- Zhu, H., Han, J., Xiao, J. Q., and Jin, Y. (2008). Uptake, translocation, and accumulation of manufactured iron oxide nanoparticles by pumpkin plants. *Environ. Monit. Assess.* 10, 713–717. doi:10.1039/b805998e
- Zhu, Y., Zhang, Z., Song, X., and Bu, Y. (2021). A facile strategy for synthesis of porous Cu₂O nanospheres and application as nanozymes in colorimetric biosensing. *J. Mater. Chem. B* 9, 3533–3543. doi:10.1039/d0tb03005h
- Živković, A., King, H. E., Wolthers, M., and De Leeuw, N. H. (2021). Magnetic structure and exchange interactions in pyrrhotite end member minerals: hexagonal FeS and monoclinic Fe₇S₈. *J. Phys. Condens. Matter* 33, 465801. doi:10.1088/1361-648X/ac1cb2
- Zuo, Y., and Deng, Y. (1999). Evidence for the production of hydrogen peroxide in rainwater by lightning during thunderstorms. *Geochim. Cosmochim. Acta* 63, 3451–3455. doi:10.1016/s0016-7037(99)00274-4

Glossary

•O₂*	superoxide radicals	IspH	(E)-4-hydroxy-3-methylbut-2-enyl pyrophosphate reductase
α-Fe₂O₃	Hematite	k_{cat}	Catalytic constant
γ-Fe₂O₃	Maghemite	K_m	Michaelis-Menten constants
2L-Fht	2-line ferrihydrite	Lc	Laccase
6L-Fht	6-line ferrihydrite	Lep	lepidocrocite
AKA	akageneite	LUCA	Last universal common ancestor
AOx	Alcohol oxidase	MoS₂	Molybdenum disulfide
ATP	adenosine triphosphate	Ms	Magnetization of saturation
CAT	Catalase	MTB	Magnetotactic bacteria
CeO₂	Ceria	NEXAFS	Near Edge X-ray Absorption Fine Structure
CeVO₄	Cerium vanadate	NPs	Nanoparticles
Cyt c	Cytochrome c	NWs	Nanowires
DAB	diazoaminobenzene	O₂	molecular oxygen
DET	Direct electron transfer	OPD	o-phenylenediamine
DFT	Density function theory	OXD	Oxidase
DNA	Deoxyribonucleic acid	POD	Peroxidase
DPD	N, N-diethyl-1,4-phenylenediamine	ROS	Reactive oxygen species
EPR	Electron paramagnetic resonance	Sch	Schwertmannite
ET	Electron transfer	SAED	Selected area electron diffraction
ETp	Electron transport	SEM	Scanning electron microscope
Fe_{1-x}S	Pyrrhotite	SOD	Superoxide dismutase
FeO	Wustiteite	SOE	Sulfite oxidase
Fe-O	Iron is bonded with oxygen atoms, such as iron oxides (e.g., hematite, magnetite) or other iron-oxygen complexes	TEM	Transmission electron microscopy
Fe₃O₄	Magnetite	TMB	3,3,5,5-tetramethylbenzidine
Fe₃S₄	Greigite	Trp	tryptophan
Fe₉S₁₁	Smythite	Tyr	tyrosine
FeS	Mackinawite	V₂O₅	Vanadium pentoxide
Fe-S	Iron is bonded with sulfur atoms, such as iron sulfides (e.g., pyrite, Pyrrhotite) or other iron-sulfur complexes	XAFS	X-ray absorption fine spectroscopy
FeS_{2m}	Marcasite		
FeS_{2p}	Pyrite		
Foh	Feroxyhyte		
Goe	Goethite		
GOE	Great oxidation event		
Gox	Glucose oxidase		
GPx	Glutathione peroxidase		
H₂O₂	Hydrogen peroxide		
His	Histidine		
HRP	Horseradish peroxidase		
HRTEM	High-resolution transmission electron microscopy		